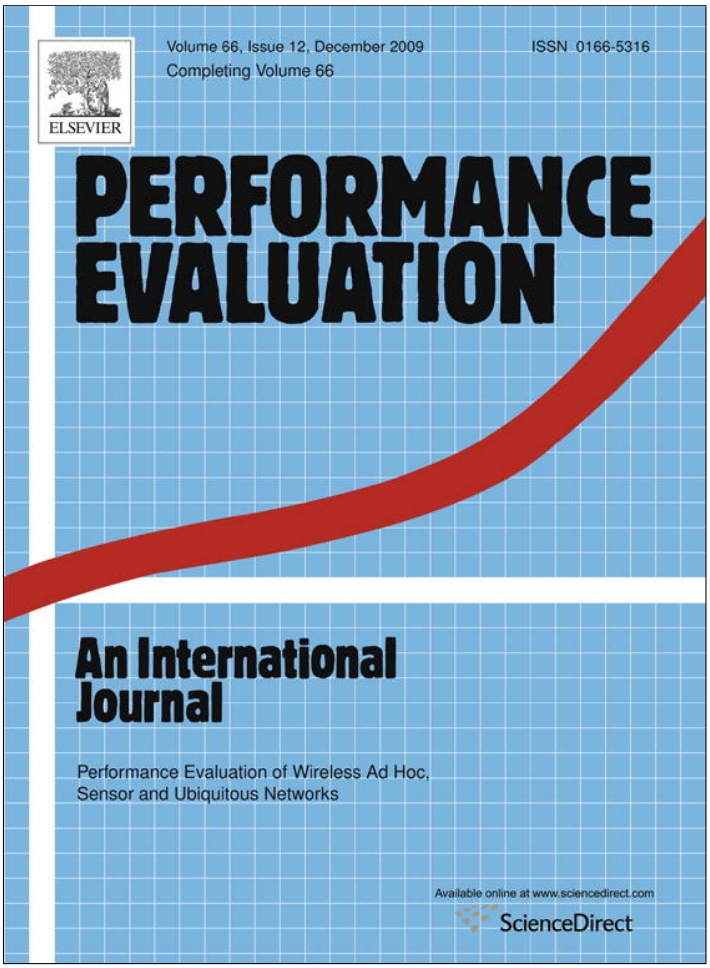

Performance Evaluation 66 (2009) 722–741

Contents lists available at ScienceDirect

Performance Evaluation

journal homepage: www.elsevier.com/locate/peva

Markov Chain-based performance analysis of multihop IEEE 802.15.4 wireless networks☆

Marco Martalò *, Stefano Busanelli, Gianluigi Ferrari

Wireless Ad-hoc and Sensor Networks (WASN) Laboratory, Department of Information Engineering, University of Parma, Italy

ARTICLE INFO

Article history:
Received 1 December 2008
Received in revised form 6 July 2009
Accepted 6 August 2009
Available online 21 August 2009

Keywords:
Markov chains
IEEE 802.15.4
Relay
Buffer
Medium access control (MAC) protocol
Cluster-tree (CT) networks

ABSTRACT

In this paper, we propose a Markov chain-based analytical framework for modeling the behavior of the medium access control (MAC) protocol in IEEE 802.15.4 wireless networks. Two scenarios are of interest. First, we consider networks where the (sensor) nodes communicate directly to the network coordinator (the final sink). Then, we consider cluster-tree (CT) scenarios where the sources communicate to the coordinator through a series of intermediate relay, which forward the received packets and do not generate traffic on their own. In both scenarios, no acknowledgment messages are used to confirm successful data packet deliveries and communications are beaconed (i.e., they rely on synchronization packets denoted as "beacons"). In all cases, our focus is on networks where the sources and the relays have finite queues (denoted as buffers) to store data packets. The network performance is evaluated in terms of aggregate network throughput and packet delivery delay. The performance predicted by the proposed analytical framework is in very good agreement with realistic ns-2 simulation results.

1. Introduction

Wireless sensor networks (WSNs) have recently received a significant attention in the research community. In particular, the development of low-power and low-cost devices makes WSNs a promising technology for the future [1]. In this context, the IEEE 802.15.4 standard has been successfully proposed [2]. An IEEE 802.15.4-compliant network comprises the following two main types of nodes: (i) a central coordinator, which initializes the network and manages its parameters; and (ii) remote sensor nodes, which collect (through sensing units) data on the status of the physical phenomena of interest and transmit them to the coordinator (acting as a sink) through (possible) multihop wireless communications. For the sake of conciseness, in the remainder of this paper the term "sensor" will be used interchangeably with "sensor node". In particular, three kinds of topologies are envisioned: (i) star, (ii) cluster-tree (CT), and (iii) mesh. The IEEE 802.15.4 standard refers to the first two layers of the ISO/OSI stack protocol, i.e., physical and Medium Access Control (MAC) layers.

Several approaches, based on simulations and experiments, have been proposed for performance evaluation of IEEE 802.15.4 networks (see, for example, [3,4] and the references therein). However, it is of interest to derive analytical tools which can be used to predict accurately the network performance without resorting to lengthy simulations or difficult experiments. Relevant network performance indicators, which will be also considered in this paper, are throughput and delay. An interesting and simple model for unsaturated traffic conditions is presented in [5]. More precisely, a Markov chain-based theoretical model is proposed to characterize both the sensors and the channel, and a good agreement with ns-2 simulations is verified [6].

☆ This paper was presented in part at the *International Symposium on Communications, Control and Signal Processing* (ISCCSP'08), St. Julians, Malta, March 2008, and at the *International Symposium on Spread Spectrum Techniques and Applications* (ISSSTA'08), Bologna, Italy, August 2008.

* Corresponding author.
E-mail addresses: martalo@tlc.unipr.it (M. Martalò), busanelli@tlc.unipr.it (S. Busanelli), gianluigi.ferrari@unipr.it (G. Ferrari).

0166-5316/$ – see front matter © 2009 Elsevier B.V. All rights reserved.
doi:10.1016/j.peva.2009.08.011

In this paper, we combine the theory of Discrete Time Markov Chains (DTMCs), considered in [5], and the theory of Geo/G/1/L queues [7], in order to derive a DTMC-based analytical model for an IEEE 802.15.4 network, which takes into account the presence of buffers (and their sizes) at the sources and the relays. More specifically, given a group (a "cluster") of nodes with the same characteristics, we focus on one of them, denoted as *tagged node*, using an approach similar to that followed in [8,9] for single-hop networks. This underlies the assumptions that all nodes behave, on average, in the same way and, therefore, characterizing the behavior of one of them is sufficient. Moreover, our framework can be applied for evaluating the performance of multihop networks with arbitrarily complex topologies (e.g., CT networks), where the relays may contend the shared medium access to the sources. Our Markov chain-based framework allows to evaluate the aggregate network throughput and the packet delivery delay.[1] Due to the approximations needed to make the multihop analysis tractable, in the 1-hop case our more general model is slightly less accurate than other, such as those proposed in [10–13], expressly designed only for these specific scenarios. However, the performance predicted by our analytical model is in very good agreement with the results obtained through extensive (and realistic) ns-2 simulations.

This paper is structured as follows. In Section 2, we briefly discuss about the huge literature body on performance analysis of IEEE 802.15.4 networks. In Section 3, we provide the reader with a quick overview of the IEEE 802.15.4 standard. Section 4 contains the derivation of the novel analytical models for the considered networking schemes: we start from single-hop networks to end with generic CT networks with buffers at the nodes. In Section 5, numerical results obtained with the proposed analytical models are shown and their very good agreement with realistic ns-2 simulation results is discussed. Finally, concluding remarks are given in Section 6.

2. Related work

In [14], the author proposes an analytical framework, based on a Markov chain characterization of the MAC protocol, for saturated IEEE 802.11 networks [15]. Based on this pioneering work, several approaches have been proposed for the characterization of the MAC performance of slotted IEEE 802.15.4 networks with star topologies [16]. All the works based on [14] are characterized by the fact that they focus on IEEE 802.15.4 saturated networks with star topologies, taking into account the acknowledgment (ACK) messages and the consequent retransmissions [10,11,17]. However, the assumption of saturated conditions is not realistic for WSN applications. In [13], the authors propose a new model for similar scenarios, also making a comparison with the existing ones.

While the aforementioned works do not consider the active/inactive period of the IEEE 802.15.4 nodes, this aspect is investigated in [12,18,19]. In [18], the authors assume unsaturated traffic and source nodes with a finite buffer, but only uplink communications. In [19], instead, downlink communications are also taken into account, but nodes are assumed to be equipped with infinite size buffers. In [12], it is shown that the models in [18,19], although very detailed, fail to couple with realistic simulation results. In [20], the authors analyze, beyond the throughput performance, the energy consumption in a star topology.

In [21], we have extended the framework proposed in [5] to simple 2-hop network scenarios, where sensors communicate with the coordinator through an intermediate *relay* node, which simply forwards the data packets received from the sources. As in [5], in [21] as well all the network nodes (both sensors and relay) are assumed to have no finite buffers. In [22], a finite size buffer is taken into account to generalize the framework proposed in [21]. This model has the advantage to be much simpler that the previous attempts to model finite buffer network nodes [18]. Finally, in [23,24] the authors propose the use of a relay for interconnecting two different clusters in IEEE 802.15.4 networks and analyze the performance through a queuing theoretic analysis. However, the scenarios proposed in [23,24] model simple cases where the relay does not contend the medium access to the sensors.

3. IEEE 802.15.4 standard overview

The IEEE 802.15.4 standard refers to the first two layers of the ISO/OSI stack (i.e., physical and MAC) and guarantees (in principle) a transmission data rate equal to 250 kpbs in a wireless communication link. The IEEE 802.15.4 networks can operate in two modes: asynchronous, denoted as "unslotted", and fully synchronized, denoted as "slotted". Since the main goal of an IEEE 802.15.4 network is data transmission under the constraint of maximum power saving, the slotted mode is the most appealing and is the one that has received the largest attention from the scientific community. In the slotted mode, the nodes share a common time reference provided by the coordinator. Two consecutive synchronization packets, denoted as "beacons", delimit a so-called "superframe" (shown in Fig. 1), which is further divided into two regions, referred to as active and inactive, respectively. While in the latter region all nodes go to the sleeping state to preserve their battery energies, in the former region all nodes can transmit their data packets. During the active region, two different access techniques can be selected, to be used in dedicated periods of variable durations. More specifically, during the Contention Access Period (CAP) every node can transmit according to a slotted non-persistent Carrier Sense Multiple Access with Collision Avoidance (CSMA/CA) MAC protocol, with the use of a proper Binary Exponential Backoff (BEB) algorithm. In the Contention Free Period (CFP), instead, only nodes with a reserved time slot, denoted as Guaranteed Time Slot (GTS), can transmit data packets, so

[1] In the remainder of this paper, the aggregate network throughput and the packet delivery delay will be simply referred to as throughput and delay, respectively.

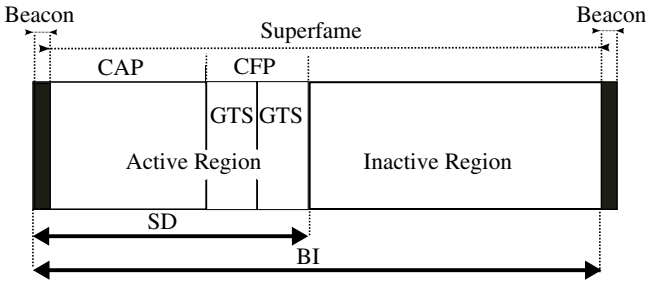

Fig. 1. Superframe structure of IEEE 802.15.4.

that collisions are avoided. To limit the complexity of the model, we set to zero the duration of the CFP, so that the structure of the superframe is completely determined by the following parameters.

- The duration of the superframe, expressed in terms of numbers of symbol durations, which can assume values in the set $\{0, 1, \ldots, 14\}$ and is proportional to 2^{BO}, where BO is the beacon order.[2]
- The duration of the active period, which can assume values in the set $\{0, 1, \ldots, 14\}$ and is proportional to 2^{SO}, where SO is the superframe order.

These values are chosen by the coordinator and notified to the other nodes through the beacon packets. Unlike [19], we do not consider the presence of an inactive region (hence, BO = SO) and the use of ACK messages. Finally, in order to further reduce the complexity in both the analytical framework and in the simulations we ignore the InterFrame Space (IFS), which is a pre-defined waiting time between two consecutive transmission acts. However, our framework can be easily extended to take into account the presence of the IFS.

The used (slotted) CSMA/CA MAC protocol relies on a discretization of the time into (backoff) slots, each with a length equal to 20 times the duration of a physical symbol. Every node can attempt to get control of the channel for a maximum number of times, denoted as m. The default value of m is 4. Before the kth attempt, the node has to wait for a random waiting time, denoted as W_k, whose length (expressed in terms of time slots) is uniformly distributed in the set $\left\{0, 1, 2, \ldots, 2^{BE_k} - 1\right\}$, $k = 1, \ldots, m + 1$, where the variables $\{BE_k\}$ are generated according to the following rule:

$$BE_{k+1} = \min\left\{BE^{min} + k, BE^{max}\right\} \quad k = 0, \ldots, m.$$

In the IEEE 802.15.4 standard, the default values BE^{min} and BE^{max} are fixed to 3 and 5, respectively.

At the end of the kth waiting period, the node assesses the status of the channel through a Clear Channel Assessment (CCA) operation during the first 8 time symbols of the successive slot. If the channel is busy and the kth attempt fails, the node will start the waiting time of the $(k+1)$th backoff cycle (if $k + 1 \leq m$); otherwise, the node will perform a second CCA operation in the successive slot. We denote as the kth backoff cycle the union of the kth double CCA operations and the kth waiting time. Since in our model the time unit is given by a backoff slot, we ignore the time needed by the transceiver to switch between transmission and reception modes—this time has to be shorter than 12 time symbols. Finally, observe that even if the channel access attempt succeeds, the transmission can be delayed to the successive superframe if in the current one there is not enough time to complete the transmission.

4. Markov Chain-based models

The scenarios of interest for 1-hop and 2-hop networks are shown in Fig. 2(a) and Fig. 2(b), respectively. All nodes have a finite dimension buffer (at the MAC level), with the exception of the sink, which is assumed to have an infinite buffer. The number of sources is denoted as M. Our analytical model allows to choose independently the buffer sizes of relay and sources. However, due to some limitations of the network simulator and for the sake of simplicity, all buffer sizes are fixed to the same value, denoted as L. While 1-hop and 2-hop networks are considered in Section 4.1 and Section 4.2, respectively, in Section 4.3 we extend our approach to more complicated CT networks.

4.1. Single-hop network scenarios

Our analytical model is a direct extension of that proposed in [5] for "bufferless" scenarios. In this case, there is no queue for storing packets waiting to be scheduled for transmission and a generated packet can be stored at the node only if no other packet is currently stored. For the sake of clearness, we now summarize the main assumptions behind our model. The simulation results will confirm the validity of these assumptions.

- All the sources generate traffic according to the same distribution. Therefore, as anticipated in Section 1, it is possible to study a "tagged" node to characterize all source nodes [9].
- As stated in Section 3, if the remaining time in the current superframe is not sufficiently long for a data packet transmission to be completed, the node must defer it to the next superframe. When the duration of the superframe is

[2] Note that the value BO = 15 is used for the unslotted mode [2].

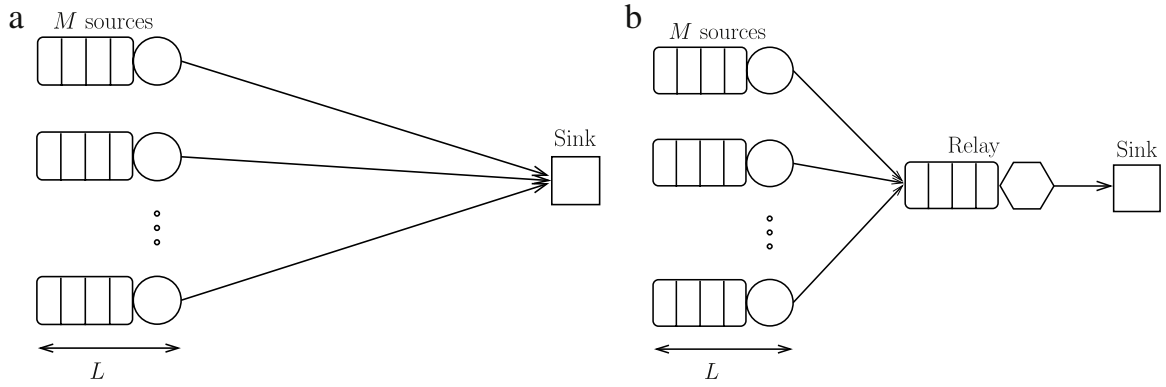

Fig. 2. Network scenarios of interest for (a) 1-hop and (b) 2-hop communications.

sufficiently long and the traffic load is not too high, the above situation rarely appears and, therefore, will be neglected in our analytical model. Clearly, if the value of BO is too small this assumption is no longer valid. In particular, the analytical model will be shown to be accurate for values of BO larger than 5.

- The probability that the channel is sensed idle in a given backoff slot is approximated by the steady-state probability that the channel is idle. This assumption has already been considered in the literature [25]. We remark that the channel idleness in one slot is not independent of that in the consecutive slot, and this will be taken into account in our model.
- The probability that a node begins its transmission in a generic slot is approximated by the steady-state probability that a node transmits.

On the basis of these assumptions, it is possible to identify two Semi-Markov Processes (SMPs): one for the shared radio channel and one for the tagged node. The presence of SMPs simplifies our derivation. In fact, it is well known that an SMP always embeds a DTMC. Moreover, if an SMP is positive recurrent, irreducible, and aperiodic, it is sufficient to know the average sojourn time of every state of the SMP and the limiting distribution of the embedded DTMC to compute the average fraction of time that the SMP spends in each state [26]. The proof of the existence of the SMP is trivial. In fact, once the embedded DTMCs are introduced, one can observe that the sojourn time of the parent process in each state is deterministic and, therefore, the parent process is a positive recurrent, irreducible, and aperiodic SMP.[3] Therefore, we can accurately model the system behavior by studying the embedded DTMCs of the channel and of the tagged node. These DTMCs are mutually coupled, as will be shown later.

4.1.1. Tagged node DTMC

The following assumptions, which lead to a simplification and an extension of the original node model presented in [5], are introduced.

- We switch from a continuous to a discrete time regime.
- We simplify the tagged node DTMC by removing a few states (namely, five states), as will be shown below.
- A finite size buffer is inserted at the MAC level of the tagged node.

In Fig. 3, the original DTMC model proposed in [5] (case (a)) is directly compared with our simplified model (case (b)). In all cases, the tagged node is bufferless. Referring to Fig. 3(a), we first describe the original model introduced in [5]. The bufferless node remains in the IDLE state until the arrival of a new packet, and the probability of a packet arrival in a single slot is denoted as p. In fact, traffic characterized by a Poisson distribution with parameter pN over N slots roughly corresponds to generating a packet, in a single slot, with probability p. When a packet is generated the node begins its first backoff cycle. In general, the workflow of the CSMA/CA MAC protocol mechanism is modeled with a series of states labeled as $\{\mathrm{BO}_k\}$, $\{\mathrm{CS}_{1k}\}$ and $\{\mathrm{CS}_{2k}\}$, where $k \in \{1, \ldots, m+1\}$ denotes the backoff cycle. In particular, during the waiting period of the kth backoff cycle the node remains in the state BO_k, e.g., after the reception of a packet the node moves into the state BO_1 from the IDLE state. The probability p_k^{n} corresponds to the parameter of the geometric distribution used in [5] to approximate the uniform distribution of the waiting period W_k. At the end of the kth waiting period, the node moves to state CS_{1k}, which models the first CCA operation. If the channel is sensed idle during the first CCA operation, the node moves from state CS_{1k} to state CS_{2k}, i.e., performs the second CCA operation. Due to the assumptions listed at the beginning of Section 4.1, this happens always with the same probability, which is denoted as $p_{\mathrm{i}}^{\mathrm{c}}$, where the subscript "i" stands for idle and the superscript "c" for channel. If, on the other hand, the channel is not sensed idle in the first CCA operation, the tagged node moves from state CS_{1k} to state BO_{k+1} (if $k < m$) or to the IDLE state (if $k = m$) with probability $(1 - p_{\mathrm{i}}^{\mathrm{c}})$. Similarly, the tagged node moves to the same states from state CS_{2k}, which models the second CCA operation. If the channel is idle conditionally on the fact that it was also idle in the previous slot – and this happens with a probability denoted as $p_{\mathrm{i}|\mathrm{i}}^{\mathrm{c}}$ – the node moves to the TX state, i.e., starts

[3] A more rigorous approach, based on finding the Markov Random Sequence (MRS) embedded in the original process, can be followed [26].

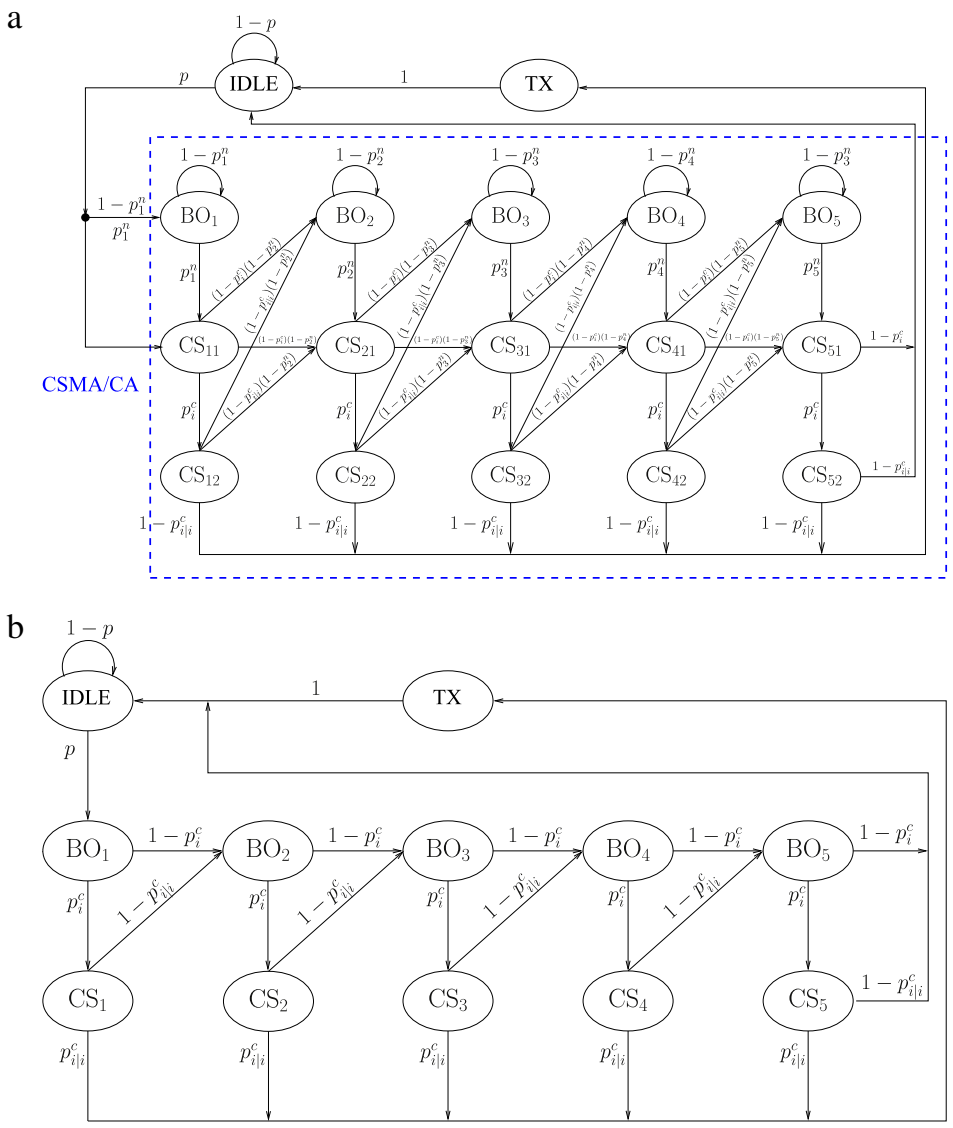

Fig. 3. Tagged node DTMC: (a) the original model from [5] and whereas (b) simplified model proposed here.

transmitting. Otherwise, the node moves to state BO_{k+1} (if $k < m$) or to the IDLE state (if $k = m$) with probability $1 - p^c_{i|i}$. The sojourn times in all states, with the exception of the TX state, are equal to one backoff slot. The transmission time, i.e., the sojourn time in the TX state, is equal to the packet size, which, in this paper, will be fixed and expressed in terms of the number of slots. For example, since at 2.4 GHz it is possible to send 10 bytes in each backoff slot, a packet size N equal to 10 means that the effective packet size is equal to 100 bytes.[4]

In the original tagged node DTMC model in [5], the presence of Poisson-distributed traffic sources is consistent with the use of a continuous time model. However, due to the slotted nature of the CSMA/CA MAC protocol and having fixed the packet duration to a multiple of the backoff slot, by considering (per slot) Bernoulli traffic sources it is possible to study the system with a fully discrete time model. Since both traffic generation models (Poisson and Bernoulli) are memoryless, the semi-Markov property of the source traffic process still holds and, therefore, the DTMC model is still valid. In particular, while in [5] the parameter of the Poisson traffic distribution is equal to pN (as mentioned in the previous paragraph), in our modified version p is the parameter of the per slot Bernoulli traffic distribution. In this case, the number of arrivals in N backoff slots has a binomial distribution with parameters N and p. Therefore, the average interarrival time is equal to $1/(Np)$, as in the case with Poisson traffic distribution over N slots with parameter pN.

Upon the assumption outlined in the previous paragraph, the tagged node DTMC can be simplified as follows. In [5], the authors approximate the uniform distribution of the backoff duration with a geometric one, in order to take advantage of its memoryless property. However, this assumption can be relaxed, thus leading to a model with lower complexity, since the SMP theory states that with the knowledge of the average sojourn time $\overline{W_k} \triangleq \mathbb{E}\{W_k\}$, $k \in \{1, \ldots, m+1\}$, it is

[4] In this work, no distinction is made between useful payload and packet headers.

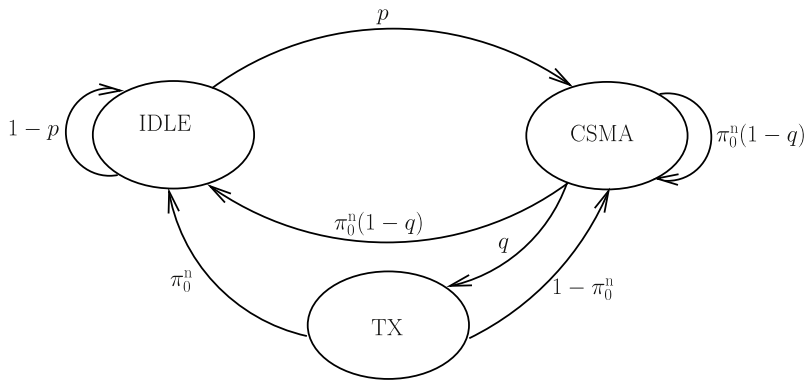

Fig. 4. DTMC model for a *buffered remote node* compliant with the IEEE 802.15.4 networks.

possible to derive the long-term behavior of the parent SMP [26]. In particular, one can remove from the original DTMC the geometric distribution approximation and the self-transition in the state $\{\mathrm{BO}_k\}$. Moreover, since the first CCA operation is always performed, one can also fuse the states BO_k and CS_{1k} of the SMP ($\forall\, k$), replacing them with a new state BO_k whose sojourn time is equal to $\overline{W_k} + 1$. Due to this reduction of the number of states and transitions in the SMP, the embedded DTMC becomes simpler as well, as shown in Fig. 3(b).

Finally, finite size buffers, all with length L, are inserted at the MAC level of sources and relay. As in classical queuing theory, L is the capacity of the entire node, formed by a queue of size $L-1$ and a server able to process one packet at a time. Therefore, a node can store L packets. The model proposed in [5] does not allow to handle the presence of a buffer with a finite size L. However, the key assumptions at the beginning of Section 4.1, namely the facts that (i) every source node has the same probability to access the channel in every time slot and (ii) the probability that the channel is idle in a certain time slot is always the same, lead to a decorrelation between the nodes' queues. Therefore, it is possible to model the queue at the tagged node as a Geo/G/1/L queue. For our purposes, we are just interested in the probability that the queue is empty after a packet departure, either successful or unsuccessful (because of a channel access failure). We denote this probability as π_0^{n}. In particular, after a packet departure, in the model in [5] the node DTMC always moves to the IDLE state. However, in the presence of a finite buffer the behavior is different. In particular, if the queue is not empty after a packet departure (with probability $1-\pi_0^{\mathrm{n}}$), the node will start again the CSMA/CA MAC protocol-based channel access mechanism, moving to state BO_1. Conversely, if the queue is empty (with probability π_0^{n}), the node moves to the IDLE state. Due to the assumptions previously made, the modifications in the node DTMC do not affect the "nature" of the process governing the behavior of a source node, i.e., this process remains an SMP. For this reason, an embedded DTMC can still be extracted. Moreover, this DTMC is ergodic, since it is irreducible, aperiodic, and finite [26]. In Fig. 4, a simplified representation of the DTMC model for the buffered tagged node is shown. Note that the macrostate CSMA embeds all the workflow of the CSMA/CA MAC protocol shown in Fig. 3(b). When π_0^{n}, $p_{\mathrm{i}}^{\mathrm{c}}$, and $p_{\mathrm{i|i}}^{\mathrm{c}}$ are known, using proper balance equations the limiting distribution of the tagged node DTMC, denoted as $\boldsymbol{\pi}^{\mathrm{n}}$, and of the long-term sojourn times of the SMP, denoted as $\boldsymbol{\Pi}^{\mathrm{n}}$, can be computed in a closed form, as shown in Appendix A.

To determine the distribution of the number of costumers in the queue of the tagged node in correspondence to a slot boundary, the expression of the packet service time is needed. This time is given by the sum of the time necessary to transmit a packet and the time spent to access the channel. Since the packet size is fixed, the distribution of the packet service time depends only on $p_{\mathrm{i}}^{\mathrm{c}}$ and $p_{\mathrm{i|i}}^{\mathrm{c}}$.

The probability generating function (PGF) of the packet service time (denoted as $T_{\mathrm{t}}(z)$) can be expressed as a function of the PGFs of the kth backoff cycle duration (denoted as $B_k(z)$) and the time necessary to transmit a packet (denoted as $T_{\mathrm{tx}}(z) = z^N$). In order to simplify the derivation of the expression of $T_{\mathrm{t}}(z)$, we ignore the time spent during the second CCA operation and we include the time spent during the first CCA operation into the waiting time, since the first CCA operation is always performed. This leads to a unitary right shift of the uniform distribution of the waiting time of a generic backoff attempt, so that $B_k(z)$ can be expressed as follows:

$$B_k(z) = z\frac{z^{2^{\mathrm{BE_k}}} - 1}{2^{\mathrm{BE_k}}(z-1)} \quad k = 1, \ldots, m+1.$$

The packet service time is given by two distinct components: the first, denoted as $T_{\mathrm{succ}}(z)$, accounts for the successfully transmitted packets, while the second, denoted as $T_{\mathrm{fail}}(z)$, accounts for the discarded packets because of a CSMA/CA MAC protocol failure. Using the approach proposed in [19], after a few manipulations, it can be shown that

$$T_{\mathrm{t}}(z) = \underbrace{T_{\mathrm{tx}}(z)p_{\mathrm{i}}^{\mathrm{c}}p_{\mathrm{i|i}}^{\mathrm{c}}\sum_{k=1}^{m+1}\left(1-p_{\mathrm{i|i}}^{\mathrm{c}}p_{\mathrm{i}}^{\mathrm{c}}\right)^{k-1}\prod_{j=1}^{k}B_j(z)}_{T_{\mathrm{succ}}(z)} + \underbrace{\left(1-p_{\mathrm{i|i}}^{\mathrm{c}}p_{\mathrm{i}}^{\mathrm{c}}\right)^{m+1}\prod_{j=1}^{m+1}B_j(z)}_{T_{\mathrm{fail}}(z)}. \quad (1)$$

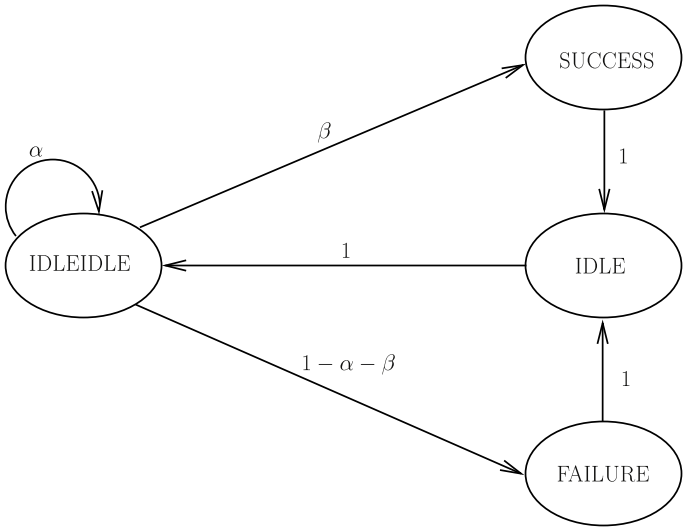

Fig. 5. DTMC model for the *physical communication channel* in IEEE 802.15.4 networks.

We now give insights on expression (1) for $T_t(z)$, characterizing the two terms $T_{succ}(z)$ and $T_{fail}(z)$.

- A successfully transmitted packet has to find the channel free for two consecutive CCA operations. This happens with the same probability in every backoff cycle, namely with probability $p^c_{i|i}p^c_i$. It is clear that the node will transmit at the kth backoff cycle ($k \leq m+1$) if it failed all previous $k-1$ attempts, and this happens with probability $\left(1-p^c_{i|i}p^c_i\right)^{k-1}$. The waiting time of the packet is given by the sum of the waiting time in all backoff cycles in which the packet unsuccessfully attempted to access the channel. Therefore, we can express the PGF of the waiting time of the packet transmitted during the kth backoff cycle as $\prod_{j=1}^{k} B_j(z)$. In each possible successful transmission scenario, the multiplicative term $T_{tx}(z)$ takes into account the packet transmission time.
- Instead, the term $T_{fail}(z)$ can be derived in an easier manner. A discarded packet has to attempt without success during all the $m+1$ backoff cycles, and this happens with probability $\left(1-p^c_{i|i}p^c_i\right)^{m+1}$. In this case, the waiting time is given by the term $\prod_{j=1}^{m+1} B_j(z)$.

From (1), using the procedure described in [7] and reported in Appendix A, one can derive the distribution of the number of customers that are queued at the time of a packet departure. This vector of size L is denoted by $\boldsymbol{\pi}^n = [\pi^n_0\pi^n_1\cdots\pi^n_{L-1}]$, where π^n_k is the probability that the queue of the tagged node contains k packets immediately after a packet departure ($k \in \{0, 1, \ldots, L-1\}$).

4.1.2. Channel DTMC

In Fig. 5, the DTMC model for the physical communication channel is shown. As one can see, in this case there are four states, denoted as IDLEIDLE, SUCCESS, IDLE, and FAILURE. The first state of the channel DTMC is denoted as IDLEIDLE, because before every transmission the channel has to remain idle for two consecutive slots, as stated by the IEEE 802.15.4 standard [2]. When a new packet is transmitted, the channel schedules a new transmission with probability $1-\alpha$, where $\alpha \triangleq (1-p_{t|ii})^M$ is the probability that no source has transmitted given that the channel was idle during the two previous slots, $p_{t|ii}$ is the probability that the tagged node transmits given that the channel was idle during the two previous slots, and M is the number of sources. Using the Bayes theorem, the probability $p_{t|ii}$ can be expressed as follows:

$$p^n_{t|ii} = \frac{p^n_t}{p^c_{ii}} \tag{2}$$

where p^n_t can be obtained from the limiting distribution $\boldsymbol{\pi}^n$ of the tagged node DTMC, multiplying the long-term sojourn times in the states $\{CS_{i2}\}_{i=1}^{5}$ by the probability of finding the channel free in the second CCA, which is given by [5]

$$p^n_t = \left(\frac{\sum_{i=1}^{m+1}\pi^n_{CS_{i2}}}{\pi^n_I + N\pi^n_{TX} + \sum_{i=1}^{m+1}\pi^n_{CS_{i2}} + \sum_{i=1}^{m+1}\left(\overline{W_k}+1\right)\pi^n_{BO_i}}\right)\frac{1}{p^c_{i|i}}.$$

Conversely, if just a single node transmits, the channel moves to the SUCCESS state: this event happens with probability $\beta \triangleq Mp^n_{t|ii}(1-p^n_{t|ii})^{M-1}$. Finally, if more than one nodes transmit at the same time, the channel moves to the FAILURE state: the probability of this event is clearly $1-\alpha-\beta$. After a packet transmission has been carried out, either successfully or

unsuccessfully, the channel moves to the IDLE state with probability 1 and then[5] to the IDLEIDLE state with probability 1. Given the values of α and β (obtained by solving the tagged node DTMC), it is possible to derive the closed-form limiting distribution of the channel DTMC, denoted as $\boldsymbol{\pi}^{\mathrm{c}}$, and of the long-term sojourn times of the SMP, denoted as $\boldsymbol{\Pi}^{\mathrm{c}}$, as shown in Appendix B. In particular, given $\boldsymbol{\Pi}^{\mathrm{c}}$, it possible to compute both $p_{\mathrm{i}}^{\mathrm{c}}$ and $p_{\mathrm{i|i}}^{\mathrm{c}}$ as follows:

$$p_{\mathrm{i}}^{\mathrm{c}} = \Pi_{\mathrm{II}}^{\mathrm{n}} + \Pi_{\mathrm{I}}^{\mathrm{n}} = \frac{2-\alpha}{1+(N+1)(1-\alpha)}$$

$$p_{\mathrm{i|i}}^{\mathrm{c}} = \frac{\Pi_{\mathrm{II}}^{\mathrm{n}}}{p_{\mathrm{i}}^{\mathrm{c}}} = \frac{1}{2-\alpha}$$

where $\Pi_{\mathrm{II}}^{\mathrm{n}}$ and $\Pi_{\mathrm{I}}^{\mathrm{n}}$ are the long-term sojourn times in the IDLEIDLE and IDLE states, respectively. Note that we are implicitly assuming that every node sees itself as a "competitor" for accessing the channel. Clearly, this is unrealistic, since in a real network a node cannot compete with itself. However, this assumption is expedient to allow us to extend our analytical model to scenarios with multihop communications or heterogeneous networks, i.e., where nodes or group of nodes may have different medium access strategies.

4.1.3. Throughput and delay

As mentioned in the previous subsection, the tagged node and channel DTMCs are coupled. Their distributions can then be obtained by solving proper fixed-point equations, as explained in detail in Appendix C. Once the distributions of these DTMCs and the long-term sojourn times in the states of their parent SMPs are computed, the system performance, in terms of throughput and delay, can be evaluated as follows.

According to the formulation used in [5], the throughput coincides with the average fraction of time (over a sufficiently long time horizon) spent in the SUCCESS state by the channel SMP and is given by

$$\Pi_{\mathrm{S}}^{\mathrm{n}} = \frac{N\beta}{1+(N+1)(1-\alpha)}. \tag{3}$$

However, in order to use a common definition for both single-hop and multihop networks, we define the throughout as

$$S \triangleq M p_{\mathrm{t}}^{\mathrm{n}} (1 - p_{\mathrm{t|ii}}^{\mathrm{n}})^{M-1} \tag{4}$$

where $p_{\mathrm{t}}^{\mathrm{n}} = \Pi_{\mathrm{TX}}^{\mathrm{n}}$ is the fraction of time spent by the tagged node SMP in the TX state and is given in Appendix A, while $p_{\mathrm{t|ii}}^{\mathrm{n}}$ is given by Eq. (2). Eq. (4) simply states that the aggregate network throughput is given by the fraction of time spent by a single node in the TX state multiplied by the probability that the others $M-1$ nodes do not transmit in the same slot. We remark that in 1-hop scenarios, our definition (4) for the throughput leads to the same result obtained using the definition proposed in [5] and given by (3).

In the computation of the delay, we will take into account only the packets which successfully access the channel through the CSMA/CA MAC protocol mechanism. Note that we assume that the delay experienced by a collided packet is the same of a packet successfully transmitted, since we are not considering the use of ACK messages. Once the distribution of the tagged node queue at the time of a packet departure (i.e, $\boldsymbol{\pi}^{\mathrm{n}}$) is known, using Little's law the average waiting time can be computed as

$$\overline{W} = \frac{\sum_{\ell=1}^{L-1} \ell\pi_\ell + L(\pi_o + p\overline{T}_{\mathrm{t}} - 1)}{p} - \overline{T}_{\mathrm{t}} \tag{5}$$

where $\overline{T}_{\mathrm{t}} = T_{\mathrm{t}}^{(1)}(z)\Big|_{z=1}$ is the average packet service time. The packets dropped due to CSMA/CA MAC protocol failures experience a different average *service* time ($\overline{T}_{\mathrm{fail}}$) with respect to the transmitted (successfully or not) packets ($\overline{T}_{\mathrm{succ}}$). However, the average *waiting* time is the same for all packets. Therefore, from (1) and (5) one can evaluate the average delay of a successfully transmitted packet as follows:

$$\overline{D} = \overline{W} + \overline{T}_{\mathrm{succ}}. \tag{6}$$

4.2. 2-hop network scenarios with single relay

In this subsection, we show how to modify the proposed DTMC models for 1-hop scenarios, in order to take into account the presence of an intermediate relay. In [21], one can find more details about a possible model for *bufferless* scenarios. However, this model is not of practical interest, since it has been created in an ad hoc way and cannot be easily generalized. Therefore, in the following we will only present a more general model for *buffered* scenarios.

[5] One may think that the IDLE state could be merged with the IDLEIDLE state in the DTMC shown in Fig. 5. However, the presence of the IDLE state is expedient for modeling the IEEE 802.15.4 standard, where a few free time slots are inserted before a new superframe is scheduled. The presence of the IDLE state, on the other hand, simplifies also the throughput calculation.

Modeling multihop networks with buffers at the nodes is challenging for several reasons: the numbers of customers in the network queues are strongly correlated; the service time of the relay queue is correlated with the arrival process distribution (the packet dimension is fixed and every node shares the same channel); the distribution of the arrival process at the relay node cannot be easily characterized. Without proper approximations, almost every analytical model will become mathematically intractable. Roughly speaking, our modeling goal consists in reaching the best tradeoff between analytical complexity and accuracy of the results. The following assumptions are then considered.

- Due to the Geo/G/1/L queuing theory, it is possible to determine the output process of source nodes [7]. However, the arrival process at the relay is not a linear combination of the output processes of the source nodes: in fact, because of the collisions between transmitted packets, not all packet departures from the source nodes become new arrivals at the relay queue. Moreover, when the relay is involved in a CCA operation, it cannot receive any packet, regardless of its queue status [2]. To the best of our knowledge, we are not aware of any work which successfully characterizes the output process of a wireless channel using the CSMA/CA MAC protocol [9]. Therefore, we arbitrarily assume that the arrival process at the relay has a Bernoulli distribution with a parameter, denoted as p_r, which is different with respect to the parameter p of the Bernoulli traffic distribution at each source node. Since we are assuming an arbitrary Bernoulli approximation of the arrival distribution at the relay, even if it were possible to derive a closed-form expression for the first-order statistic of the output process, this value would not coincide with the desired p_r.
- Since the packet size is fixed and owing to the assumption that every node experiences the same long-term channel condition, the packet service time is assumed to be the same for relay and sources. Note, however, that the corresponding queues have different behaviors since their arrival processes are different.
- We assume that the numbers of customers in different queues are independent and, therefore, we independently determine their stationary distributions.
- The service time is independent of the arrivals. In fact, if a packet experiences a short channel access delay at the source nodes, no assumption about the channel access delay at the relay can be made.

Due to the above assumptions, we can study a 2-hop scenario by simply adding a relay DTMC equal to a source DTMC, except for a different parameter of the per slot Bernoulli traffic distribution ($p_r \neq p$). Moreover, the relay is equipped with a Geo/G/1/L queue equal to that of a source except for the arrival process parameter. Therefore, we are in the presence of three DTMCs (one for the tagged source node, one for the relay, and one for the channel) and two Geo/G/1/L queues (one for the tagged source node and one for the relay) mutually coupled. While in the 1-hop scenario there is a single unknown parameter p_i^c, there are now two unknown parameters: p_i^c and p_r. In this case, a vectorial fixed-point equation of the following form (extending the approach outlined in Appendix C.1 for single-hop scenarios) can be derived:

$$(p_i^c, p_r) = \Psi(p_i^c, p_r)$$

where $\Psi(p_i^c, p_r)$ depends on the structures of the tagged node block (DTMC and queue), the relay block (DTMC and queue), and the channel DTMC.

Upon the derivation of p_i^c and p_r, the long-term sojourn times of the SMPs of the tagged node and the relay, the throughput and delay performance of the considered networks can then be evaluated. As in Section 4.1.3, here as well we define the throughput S as

$$S = p_t^r (1 - p_{t|ii}^n)^M \tag{7}$$

where p_t^r is the long-term fraction of time spent by the relay in the TX state and $1 - p_{t|ii}^n$ is the probability of correct transmission (i.e., when all the M source nodes do not transmit).

The average end-to-end delay is simply obtained by adding the average delay experienced by the tagged node, denoted as $\overline{D}^n$, and the average delay experienced by the relay node, denoted as $\overline{D}^r$:

$$\overline{D} = \overline{D}^r + \overline{D}^n.$$

4.3. Cluster-tree networks

We now consider a general CT network, where the traffic generated at the sources (leafs) flows towards the sink (root), through a series of intermediate relays. In particular, each relay receives packets coming from a specific cluster of sources. At the same time, the relays may be grouped into higher level clusters, which can be associated with even higher level relays or by the sink itself. By grouping the sources and the relays at the various hierarchical levels, one obtains the CT network depth. For example, the network in Fig. 2(b) is a particular CT network with a depth equal to 3 and the following hierarchical levels: the first level contains $M = 12$ sources, the second level is composed by the single relay, and the last level contains just the sink. Another example of CT network topology is shown in Fig. 6, where $M = 12$ source nodes are grouped into 3 clusters (with 6, 4, and 2 sources each, respectively). The depth of this CT network is 3 and the following multihop communications to the sink are established:

- the six sources in cluster 1 reach the sink through 3-hop paths where relays 1 and 3 are used;
- the four sources in cluster 2 reach the sink through 3-hop paths where relays 2 and 3 are used;
- the two sources in cluster 3 reach the sink through 2-hop paths where relay 3 is used.

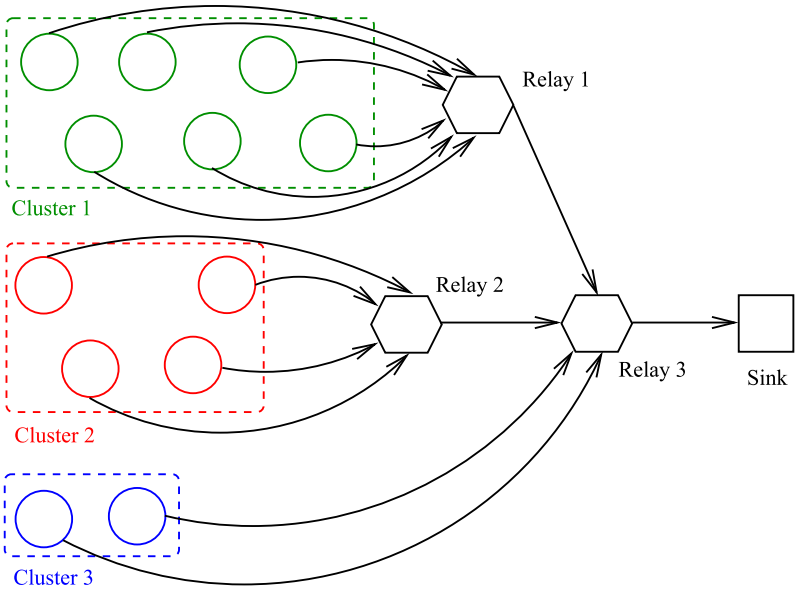

Fig. 6. Cluster-tree topology with $M = 12$ sources grouped into a CT network with 3 clusters, 3 relays, and depth equal to 3.

Following the same approach used in Section 4.2 for the two-hop networks, it is possible to extend the proposed performance evaluation framework to this more general CT scenario. In particular, we assume that all relays can be modeled with the same coupled DTMC-Geo/Geo/1/L queue block. In fact, we can state that all the relays "see", on average, the same channel and, therefore, the probability of finding the channel idle is the same for all relays. The only difference between the relays is given by the parameter of the generated Bernoulli traffic. In fact, every relay receives a different amount of traffic, which depends on the nodes in its own cluster and on the corresponding amount of generated traffic. To summarize, the tagged node and the relays can be characterized as follows.

- As in a single-hop scenario, the sources can be characterized just modeling a single tagged node with the DTMC in Fig. 4 with per slot Bernoulli traffic parameter equal to p.
- The kth relay ($k = 1, \ldots, N_{\text{relays}}$, where N_{relays} is the number of relays in the network) can be modeled with the same DTMC of the tagged node but replacing the parameter p with a parameter $p_{\text{r}}^{(k)}$. Note that the relay DTMCs are strictly related to the network configuration: in CT networks with balanced tree architectures, the number of different relay DTMCs is equal to the number of CT levels; in CT networks with unbalanced tree architectures, instead, every relay may be characterized by its own DTMC model.

Therefore, by using the basic node structures presented in Section 4.1, one can model every CT network. It is clear that the accuracy of the analytical model reduces for increasing complexity of the CT network, because of the considered simplifying assumptions. It can be easily observed that the number of unknown parameters in a CT network with increasing complexity becomes larger and larger. In a CT network with N_{relays} relays, the number of unknown parameters is $N_{\text{relays}} + 1$, namely $\{p_{\text{r}}^{(k)}\}_{k=1}^{N_{\text{relays}}}$ and p_{i}^{c}. In this case, the following vectorial fixed-point equation needs to be solved:

$$\left(p_{\text{i}}^{\text{c}}, p_{\text{r}}^{(1)}, \ldots, p_{\text{r}}^{(N_{\text{relays}})}\right) = \Theta\left(p_{\text{i}}^{\text{c}}, p_{\text{r}}^{(1)}, \ldots, p_{\text{r}}^{(N_{\text{relays}})}\right)$$

where $\Theta(\cdot)$ depends on the structures of the tagged node block (DTMC and queue), the relays' blocks (DTMC and queue), and the channel DTMC. Finally, in a general CT network it becomes very difficult to prove the existence and the uniqueness of the solution of the fixed-point equation. Since the performance results predicted by our own DTMC-based system are in a very good agreement with realistic ns-2 simulation results, we are confident of the validity of our analytical framework.

5. Numerical results

We now evaluate the performance of IEEE 802.15.4 wireless networks with the proposed Markov chain-based analytical models, verifying them through extensive ns-2 simulations. After introducing the simulation set-up in Section 5.1, the system performance is evaluated in two directions. First, the CSMA/CA MAC protocol parameters are set to their default values ($m = 4$, $\text{BE}^{\text{min}} = 3$, and $\text{BE}^{\text{max}} = 5$) and the system performance is investigated by varying the network topology (Section 5.2). Then, the network topology is fixed and the system performance is evaluated by varying the CSMA/CA MAC protocol parameters (Section 5.3).

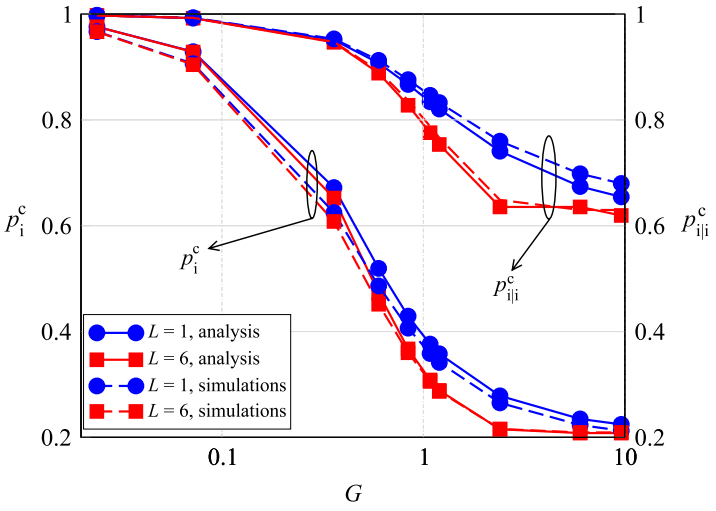

Fig. 7. p_i^c and $p_{i|i}^c$ as functions of the normalized aggregate offered load, in a scenario with 1-hop communications and $M = 12$. Two possible values for the buffer length are considered: (i) bufferless ($L = 1$) and (ii) buffered $L = 6$. Both analytical (solid lines) and simulation (dashed lines) results are presented.

5.1. Simulation set-up

The simulations are performed using the built-in model, denoted as "wpan", in the version 2.31 of ns-2 [6]. In order to analyze the scenarios of interest, we apply some modifications to the original source code of the simulator. In particular, we implement a Bernoulli traffic source and set up *static* routing in the CT network scenarios. Note that the CCA mechanism is slightly modified, since we think that its current ns-2 implementation is not compliant with the IEEE 802.15.4 standard specifications.[6] The traffic generation model per slot per node is Bernoulli with parameter p and each node generates packets with constant size of 100 bytes ($N = 10$ backoff slots) including the bytes of the physical and MAC layers. The duration of each simulation run is set to 1000 s and the presented results are obtained by averaging over a number of simulation runs sufficient to have a 95% confidence interval. Note that this set-up is in agreement with that considered in [5]. Throughput and delay are evaluated as functions of the aggregate offered load and for different values of the buffer length. In particular, we define the normalized (adimensional) average aggregate offered load as

$$G \triangleq M \cdot N \cdot p$$

where p, M, and N have been already introduced. Multiplying the normalized average aggregate offered load by the maximum transmission rate of IEEE 802.15.4 (i.e., 250 kb/s at 2.4 GHz) we obtain the average aggregate offered load g:

$$g = 250\, G \text{ [kb/s]}.$$

We recall that a portion of this aggregate offered load is dropped due to the finite length of the input buffer at the nodes. In the analytical case, the coupled DTMC-based system is solved numerically using Matlab [27] and, then, throughput and delay can be numerically evaluated.

5.2. Impact of network topology

In Fig. 7, p_i^c and $p_{i|i}^c$ are shown, as functions of the normalized aggregate offered load G, in a scenario with single-hop communications and $M = 12$ sources (i.e., all sources are directly connected to the sink). Two possible values for the buffer length L are considered: (i) 1 (bufferless scenario) and (ii) 6 (buffered scenario). Both analytical (solid lines) and simulation (dashed lines) results are shown. The analytical results are obtained with the model described in Section 4.1. As one can see, there is an excellent agreement between analytical and simulation results in all considered scenarios (bufferless and buffered). As a result, the approximations used in the analytical model are not critical for the evaluation of these probabilities and, therefore, of the network performance. Finally, it is straightforward to show that the values of p_i^c in the case with $L = 1$ are in agreement with those predicted by the transfer function approach described in Appendix C, as can be verified by comparing the results in Fig. 7 with those in Fig. 15.

In Fig. 8, the throughput is shown, as a function of the aggregate offered load G, in 1-hop and 2-hop communication scenarios with $M = 12$ sources. Both analytical and simulation results are obtained considering a buffer length L equal to 1 at the sources and the relay (bufferless scenario). The analytical results are obtained using the Markov chain-based models presented in Sections 4.1 and 4.2, respectively. The performance results for the 1-hop scenario are in agreement with those

[6] In particular, in the original implementation during the CCA operation a source node does not check all the 8 symbol intervals but just the symbol in the middle.

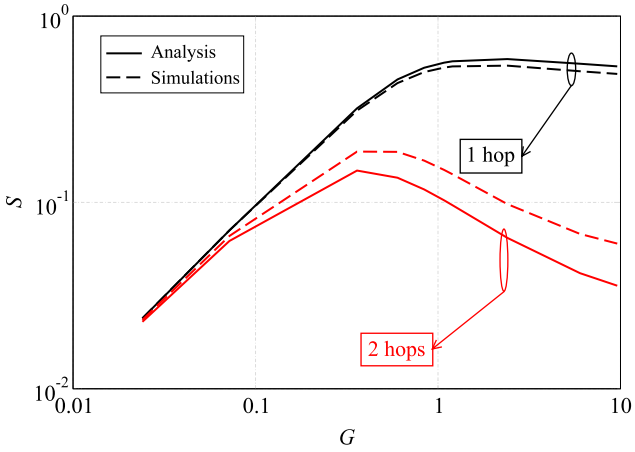

Fig. 8. Throughput, as a function of the aggregate offered load, in a scenario with $M = 12$, *bufferless* source nodes, and 1-hop and 2-hop communications to the sink. Analytical (solid lines) and simulation (dashed lines) results are shown.

presented in [5]: the throughput is rapidly increasing for small values of the offered load, whereas it very slightly decreases for large values of G. The throughput in the 2-hop scenario is lower than that in the 1-hop scenario, because (i) the time required by the transmission doubles and (ii) some packets are lost at the relay due to its finite ($L = 1$) storage capacity. In the 2-hop scenario, one can observe the presence of a well pronounced maximum, beyond which the throughput rapidly decreases. Clearly, due to the introduced approximations, there is a (small) discrepancy between analytical and simulation results. In particular, while the analytically evaluated throughput in the 1-hop scenario slightly overestimates the simulated one, in the 2-hop scenario the reversed behavior can be observed. However, one can note that the shape of the curves obtained from simulation and analytical results is exactly the same. Therefore, by using the analytical model one can predict very accurately the traffic load at which the highest throughput is reached or how the overall performance changes as a function of the traffic load.

We now investigate the impact of the buffer size at the sources and the relay. In particular, we analyze the throughput and the delay as functions of the normalized traffic load G, before combining them and deriving a classical (parameterized) throughput-delay curve. Obviously, since we are fixing the number of nodes ($M = 12$) and the packet size (100 bytes, i.e., $N = 10$ backoff slots), G depends only on p. In all considered scenarios G will assume the following values: 0.024, 0.072, 0.36, 0.6, 0.84, 1.08, 1.2, 2.4, 6, and 9.6, where $G = 0.024$ corresponds to a low traffic load condition, while $G = 9.6$ corresponds to a strong saturation condition.

In Fig. 9, the throughput (case (a)) and the delay (case (b)) are shown, as functions of the average normalized aggregate offered load G, in 1-hop scenarios. In Fig. 9(c), a family of S–D curves for 1-hop scenarios is also shown. The curves are parameterized with respect to G. Analytical (solid lines) and simulation (dashed lines) results are shown. All curves show clearly that the considered networks have a bimodal behavior. For low values of G, the delay experienced by the packets is very short and the throughput is proportional to the aggregate traffic load. In this region, the buffer length has no impact on the network performance. When the aggregate traffic load is sufficiently high, the network reaches a saturation (or unstable) regime, where the delay quickly increases and the throughput is no longer proportional to G. In the saturation region, the curves show that the dimension of the buffer has a slight impact on the throughput. In particular, its maximum and saturation values remain roughly the same—this behavior is due to the self-stability feature of the CSMA/CA MAC protocol employed by the IEEE 802.15.4 standard. A buffer length increase, instead, leads to a rapid delay increase.

In Fig. 10, we investigate the throughput-delay performance in 2-hop scenarios. Simulation (dashed lines) and analytical (solid lines) results are obtained by using, as before, two values for the (node and relay) buffer size L: (i) 2 and (ii) 5. As in 1-hop scenarios, it is possible to identify two operative regions, depending on the offered load. For low traffic load, the throughput increases proportionally to the load and the delay is bounded. In the saturation region, the throughput quickly drops and reaches very low values for high traffic loads. The relay clearly acts as a bottleneck, limiting significantly the self-stabilizing capacity of the CSMA/CA MAC protocol. Note that the performance degradation, in terms of delay, is not as pronounced as in terms of throughput. In fact, the delay is roughly twice that in the single-hop scenarios. As for 1-hop scenarios, in the considered 2-hop scenarios one can observe a very good agreement between simulation and analytical results. Therefore, the approximations introduced in Section 4.2 are meaningful.

In Fig. 11, the delay is shown, as a function of the throughput, in scenarios with (a) 1-hop and (b) 2-hop communications. In both cases, the buffer size L is set to 4. The curves are parameterized with respect to the average normalized aggregate offered load (G), which assumes the same values used in Fig. 9. Analytical (solid lines) and simulation (dashed lines) results are shown. Different values for the number of sensors M are considered: 2, 6, 10, and 18. As one can see, the model accurately predicts the network performance for sufficiently large values of M. In particular, for low values of M, e.g., $M = 2$, the trend is not well captured by our analytical framework. Otherwise, when M increases (for instance, $M \geq 6$) the trend is accurately predicted by our analytical framework. In fact, the assumptions used in the analytical derivation become valid for sufficiently large values of M. However, the typical bimodal behavior can be observed in all considered cases.

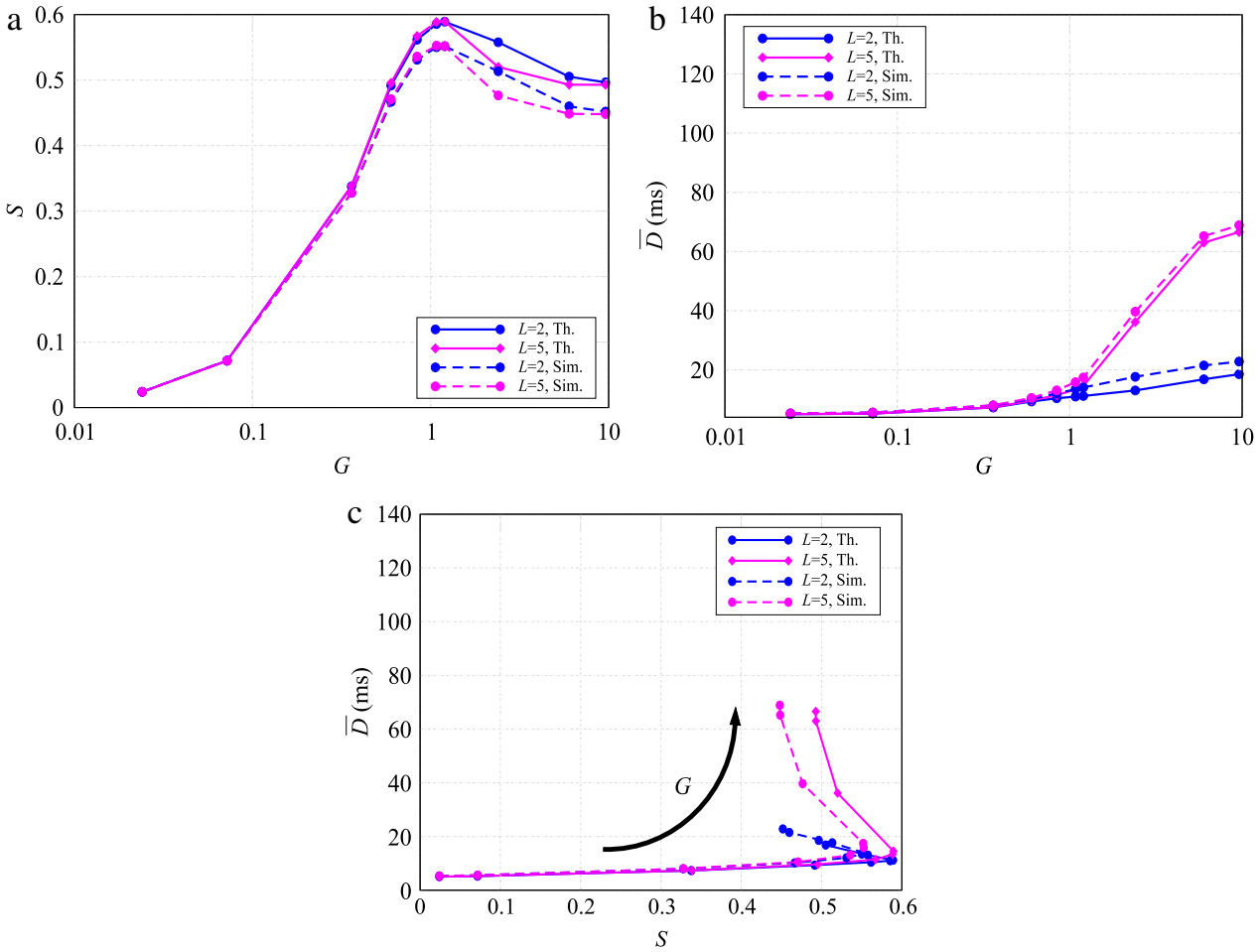

Fig. 9. Throughput (case (a)) and delay (case (b)) as functions of the average normalized aggregate offered load (G), in scenarios with 1-hop communications. In all cases, we consider $M = 12$ sources and two values of buffer size L: (i) 2 and (ii) 5. In case (c), the delay is represented as a function of the throughput. The curves are parameterized with respect to G. Analytical (solid lines) and simulation (dashed lines) results are shown.

Finally, we investigate the applicability of our model to more complicated CT network scenarios. In particular, the CT network in Fig. 6, with buffer length $L = 4$, is considered. In Fig. 12, the delay performance in this scenarios is shown as a function of the throughput. Analytical (solid lines) and simulation (dashed lines) results are presented. Two groups of curves are considered, relative to (a) per-cluster performance and (b) overall CT network performance (evaluated at the sink). Comparing Fig. 12(a) with Fig. 12(b), one can see that the overall network performance trend can be obtained by averaging over the performance curves in the various clusters. The bimodal behavior of the wireless network can be observed in each cluster. However, the maximum throughput heavily depends on the considered cluster. As one can observe, there is an excellent agreement between analytical and simulation results, especially in the stable regime, i.e., for low values of the traffic load (and delay). Therefore, one can conclude that our analytical model captures accurately the network performance trend also in CT networks with complicated topologies, where communications to the sink are carried out using multiple relays.

5.3. Impact of CSMA/CA MAC protocol parameters

In this subsection, we evaluate the accuracy of our analytical model by varying the parameters of the CSMA/CA MAC protocol. In particular, we focus on the topologies with 1-hop and 2-hop communications presented in Fig. 2, considering a finite buffer of length $L = 4$ both at the sources and relay. The CSMA/CA MAC protocol depends on four parameters: (i) BE^{min}, (ii) BE^{max}, (iii) m, and (iv) the number of CCA operations to be performed before declaring the channel idle. In [5], the authors focused on the fourth parameter, showing that in some cases the double CCA operations performed by default is a waste of time and resources. We now analyze the impact of the remaining parameters. First, the maximum number of backoff cycles is reduced to $m = 2$ (the default value is $m = 4$), in order to evaluate the performance of a network with a low delay requirement. Then, we study a network where the data reliability is more critical than the delay: in this case, we set $BE^{min} = 4$, $BE^{max} = 6$, and $m = 4$, thus increasing the average waiting time and reducing the collision probability. The model introduced in Section 4.1 can still be used, since selecting the indicated parameters only increases or reduces the number of states of the DTMC, without changing its structural properties.

In Fig. 13, the delay is shown as a function of the throughput, in scenarios with (a) 1-hop and (b) 2-hop communications. In all cases, $L = 4$, $M = 12$, and various values of m, BE^{min}, and BE^{max} are considered. The curves are parameterized with

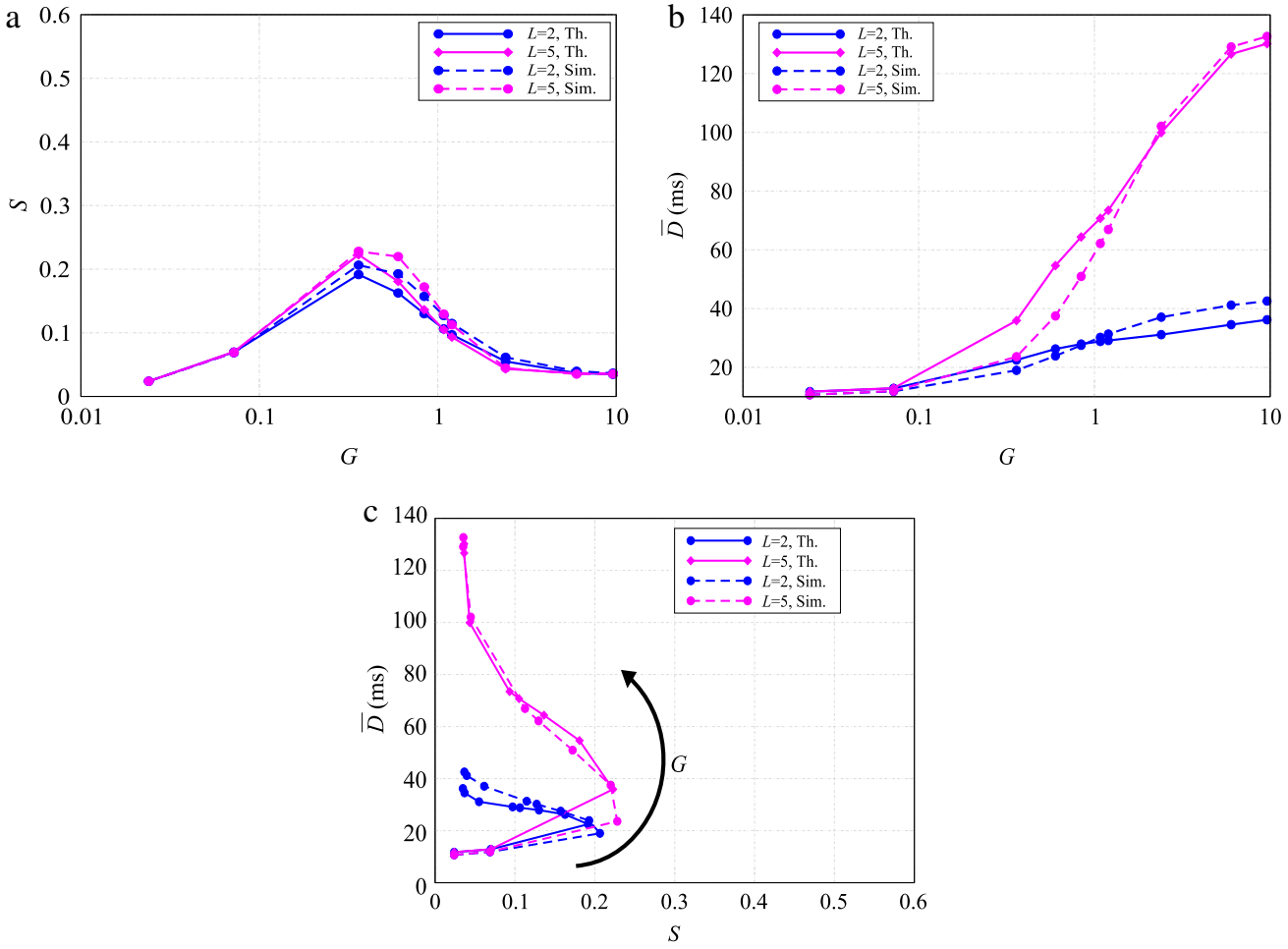

Fig. 10. Throughput (case (a)) and delay (case (b)) as functions of the average normalized aggregate offered load (G), in scenarios with 2-hop communications. In all cases, we consider $M = 12$ sources and two values of buffer size L: (i) 2 and (ii) 5. In case (c), the delay is represented as a function of the throughput. The curves are parameterized with respect to G. Analytical (solid lines) and simulation (dashed lines) results are shown.

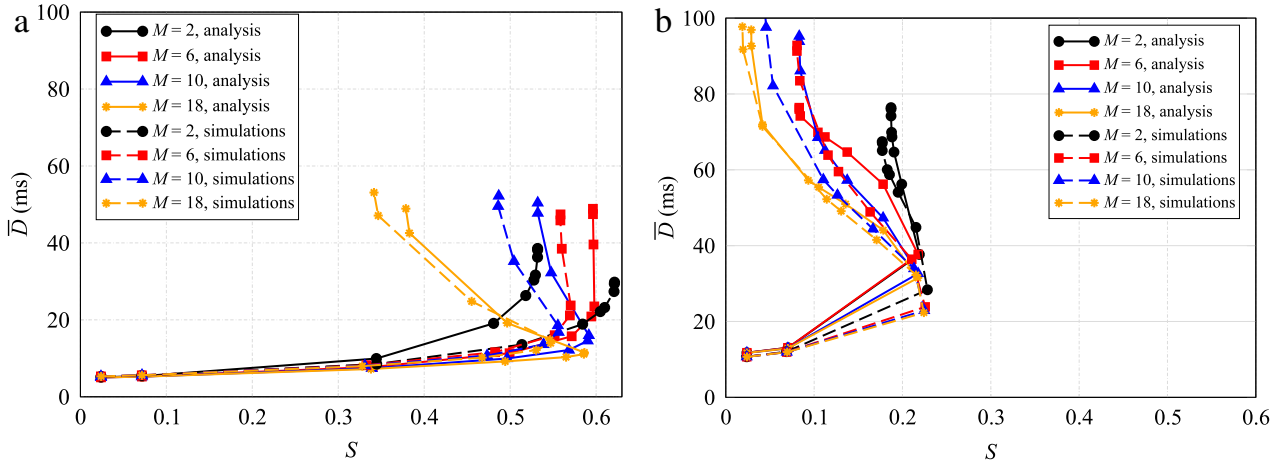

Fig. 11. Delay as a function of the throughput, in scenarios with (a) 1-hop and (b) 2-hop communications with a single relay - in both cases, $L = 4$. The curves are parameterized with respect to the average normalized aggregate offered load (G). The values of G are the same used in Fig. 9. Analytical (solid lines) and simulation (dashed lines) results are shown. Different values for the number of sensors M are considered: 2, 6, 10, and 18.

respect to the average normalized aggregate offered load (G), with the same values used in Fig. 9. Analytical (solid lines) and simulation (dashed lines) results are shown. As previously observed in Fig. 9, the considered networks have a bimodal (stable/non-stable) behavior. We remark once more the excellent agreement between analytical and simulation results in this case as well. Therefore, the approximations introduced in Section 4.2 are meaningful also for varying values of the backoff parameters (m, BE^{min}, and BE^{max}).

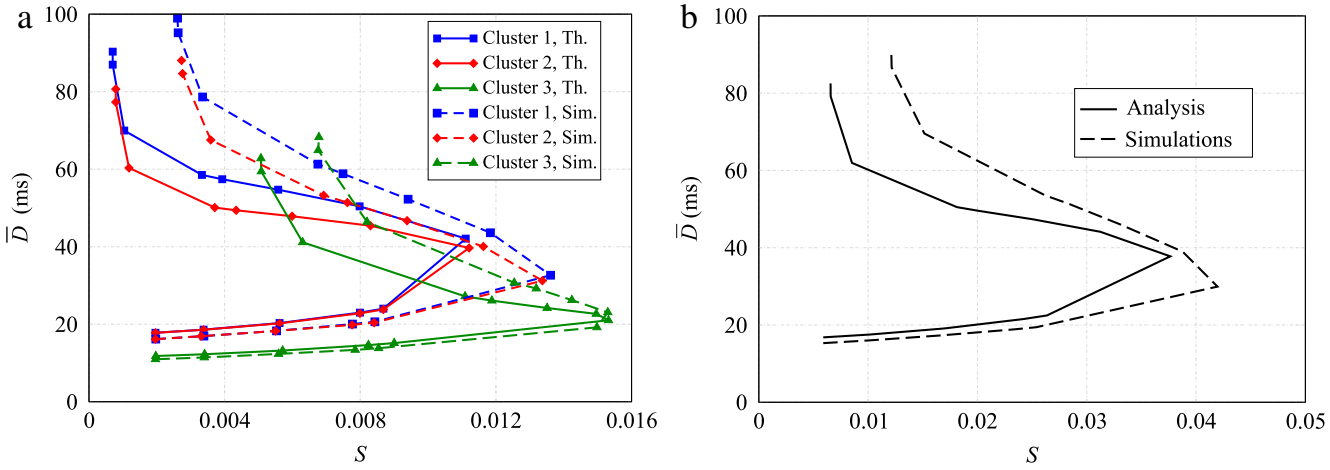

Fig. 12. Delay, as a function of the throughput, in the CT scenario depicted in Fig. 6. Two cases are considered: (a) performance for each cluster and (b) overall performance at the sink. The values of G are the same used in Fig. 9. All the nodes employs a buffer with $L = 4$. Analytical (solid lines) and simulation (dashed lines) results are presented.

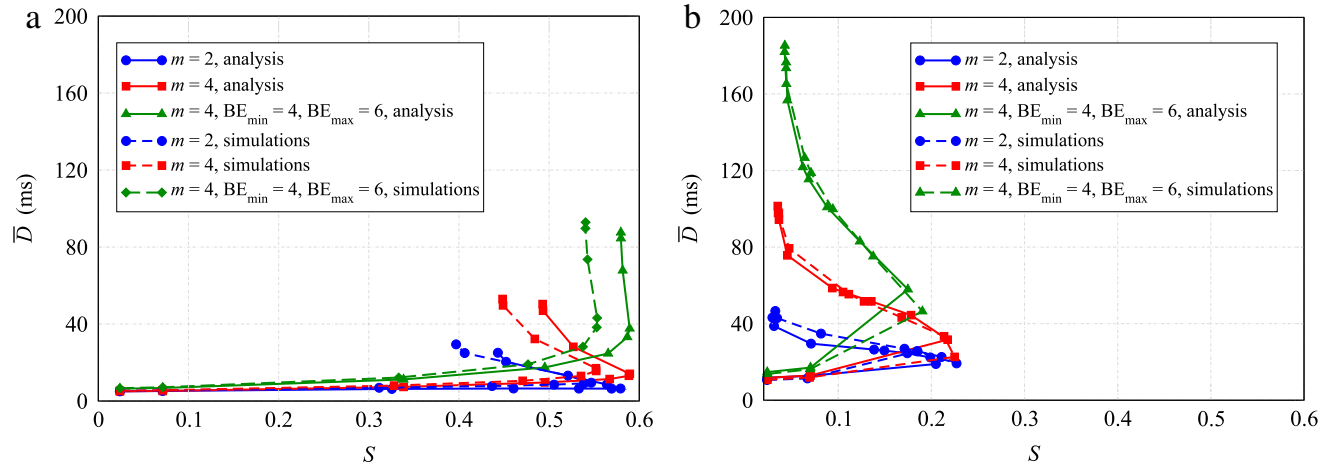

Fig. 13. Delay as a function of the throughput, in scenarios with (a) 1-hop and (b) 2-hop communications. In all cases, $L = 4$, $M = 12$, and various values of m, BE^{min}, and BE^{max} are considered. The curves are parameterized with respect to the average normalized aggregate offered load (G), with the same values used in Fig. 9. Analytical (solid lines) and simulation (dashed lines) results are shown.

6. Conclusions

In this paper, we have presented a novel analytical framework that combines the theory of DTMCs and classical queuing theory for modeling the behavior of the MAC protocol in IEEE 802.15.4 multihop wireless networks, with finite buffers at the nodes. The throughput and delay have been evaluated and the performance predicted by our analytical model is in excellent agreement with realistic ns-2 simulation results. In particular, the proposed framework is applicable to CT networks with complicated topologies and multihop communications. Our results highlight that the presence of intermediate relays drastically reduces the throughput with respect to 1-hop scenarios, i.e., the relays act as bottlenecks. This suggests that the use of relays which share the wireless medium with source nodes is not effective to extend the coverage of IEEE 802.15.4 networks. Our results depend on a large number of parameters, related to both the network topology and the MAC protocol. Therefore, our model can be applied in two directions. First, for given network topology, average packet size, number of nodes, and traffic load, one can determine the "optimal" MAC configuration which maximizes the network performance in terms of delay, throughput, or lifetime. Otherwise, one can use our analytical model to determine, for fixed MAC parameters, what is the network topology which guarantees the best performance.

Appendix A. Limiting distribution of the tagged node DTMC and long-term sojourn times of the associated SMP

First, we derive the expression of the probability that the tagged node queue is empty, i.e. π_0^n, from the PGF of the packet service time $T_t(z)$. Denoting as $a_k$the probability to have k packet arrivals into the buffer of a node during a packet service time, its PGF can be expressed, knowing the PGF of the service time $T_t(z)$, as [26]

$$A(z) = T_t(1 - p + pz)$$

from which it follows that

$$a_k = \frac{\partial^k}{\partial z^k} A(z)\bigg|_{z=0} \qquad k = 0, 1, \ldots. \tag{8}$$

Following [7], one can express the steady-state probability that a packet departure leaves k packets in the node buffer as

$$\begin{cases} \pi_k^{\mathrm{n}} = \pi_0^{\mathrm{n}} a_k + \sum_{j=1}^{k+1} \pi_j^{\mathrm{n}} a_{k-j+1} & 0 \le k \le L-2 \\ \pi_{L-1}^{\mathrm{n}} = \pi_0^{\mathrm{n}} \sum_{j=1}^{\infty} a_k + \sum_{j=1}^{L-1} \pi_j^{\mathrm{n}} \sum_{k=L-j}^{\infty} a_k \end{cases} \tag{9}$$

which can be written, by normalizing $\{\pi_k^{\mathrm{n}}\}_{k=0}^{L-1}$ with π_0^{n}, as

$$\begin{cases} \pi_0^{\mathrm{n}'} = 1 \\ \pi_{k+1}^{\mathrm{n}'} = \dfrac{1}{a_0}\left(\pi_k^{\mathrm{n}'} - \sum_{j=1}^{k} \pi_j^{\mathrm{n}'} a_{k-j+1} - a_k\right) & 1 \le k \le L-1. \end{cases}$$

Therefore, the probability of the queue to be empty is

$$\pi_0^{\mathrm{n}} = \frac{1}{\sum_{k=0}^{L-1} \pi_k^{\mathrm{n}'}}.$$

To solve the node DTMC, we write the balance equations as functions of the steady-state probability of state BO_1, i.e., $\pi_{\mathrm{BO}_1}^{\mathrm{n}}$. Defining $c \triangleq 1 - p_{\mathrm{i}}^{\mathrm{c}} p_{\mathrm{i|i}}^{\mathrm{c}}$, one obtains

$$\begin{cases} \pi_{\mathrm{BO}_\ell}^{\mathrm{n}} = c^{\ell-1} \pi_{\mathrm{BO}_1}^{\mathrm{n}} \\ \pi_{\mathrm{CS}_\ell}^{\mathrm{n}} = p_{\mathrm{i}}^{\mathrm{c}} c^{\ell-1} \pi_{\mathrm{BO}_1}^{\mathrm{n}} \\ \pi_{\mathrm{TX}}^{\mathrm{n}} = (1-c^5) \pi_{\mathrm{BO}_1}^{\mathrm{n}} \\ \pi_{\mathrm{I}}^{\mathrm{n}} = \dfrac{\pi_0^{\mathrm{n}}}{p} \pi_{\mathrm{BO}_1}^{\mathrm{n}} \end{cases} \qquad \ell = 1, \ldots, m+1 \tag{10}$$

where

$$\pi_{\mathrm{BO}_1}^{\mathrm{n}} = \left[\left(\frac{1-c^5}{1-c}\right)\left(p_{\mathrm{i}}^{\mathrm{c}} + p_{\mathrm{i}}^{\mathrm{c}} p_{\mathrm{i|i}}^{\mathrm{c}} + 1\right) + \frac{\pi_0}{p}\right]^{-1} \tag{11}$$

is derived from the normalization condition. Once obtained the limiting distribution of the DTMC, since the parent SMP is positive recurrent, irreducible, and aperiodic, its long-term sojourn times can also be found [26]. This is possible because the average sojourn times are known: in particular, they are equal to 1 for all the states with the exception of the TX state, which has an average sojourn time equal to N. The expression of the long-term sojourn time of the SMP in the TX state can be finally written as

$$p_{\mathrm{t}}^{\mathrm{n}} = \Pi_{\mathrm{TX}}^{\mathrm{n}} = \left(\frac{N\pi_{\mathrm{TX}}^{\mathrm{n}}}{\pi_{\mathrm{I}}^{\mathrm{n}} + N\pi_{\mathrm{TX}}^{\mathrm{n}} + \sum_{i=1}^{m+1} \pi_{\mathrm{CS_{i2}}}^{\mathrm{n}} + \sum_{i=1}^{m+1} \left(\overline{W_k} + 1\right) \pi_{\mathrm{BO_i}}^{\mathrm{n}}}\right). \tag{12}$$

Appendix B. Limiting distribution of the channel DTMC and long-term sojourn times of the associated SMP

In this appendix, we derive the steady-state distribution of the channel DTMC shown in Fig. 5. It is straightforward to note that the channel DTMC is ergodic and, therefore, the steady-state distribution coincides with the limiting distribution. The approach to derive the limiting distribution of the channel DTMC is the same used for a source DTMC. Leveraging on the normalization constraint and expressing the balance equations as functions of $\pi_{\mathrm{I}}^{\mathrm{c}}$, one gets the following system of four equations:

$$\begin{cases} \pi_{\mathrm{II}}^{\mathrm{c}} = \dfrac{\pi_{\mathrm{I}}^{\mathrm{c}}}{1-\alpha} \\ \pi_{\mathrm{S}}^{\mathrm{c}} = \dfrac{\beta \pi_{\mathrm{I}}^{\mathrm{c}}}{1-\alpha} \\ \pi_{\mathrm{F}}^{\mathrm{c}} = \dfrac{(1-\alpha-\beta)\pi_{\mathrm{I}}^{\mathrm{c}}}{1-\alpha} \\ 1 = \pi_{\mathrm{II}}^{\mathrm{c}} + \pi_{\mathrm{I}}^{\mathrm{c}} + \pi_{\mathrm{F}}^{\mathrm{c}} + \pi_{\mathrm{S}}^{\mathrm{c}} \end{cases}$$

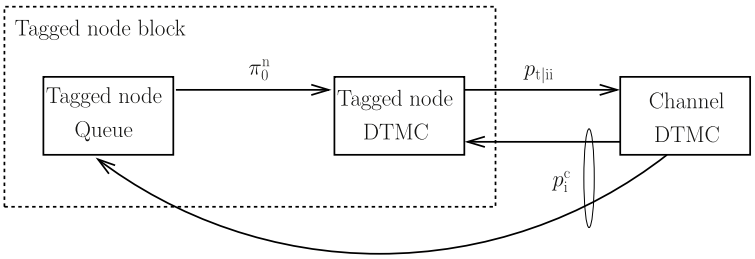

Fig. 14. Interconnection between the blocks involved in the iterative solution the non-linear fixed-point equation in single-hop scenario.

with the following (unique) solution:

$$\begin{cases} \pi_{II}^c = \dfrac{1}{3-2\alpha} \\ \pi_I^c = \dfrac{1-\alpha}{3-2\alpha} \\ \pi_S^c = \dfrac{\beta}{3-2\alpha} \\ \pi_F^c = \dfrac{1-\beta-\alpha}{3-2\alpha}. \end{cases}$$

Once the limiting distribution of the DTMC is computed, since the parent SMP is positive, recurrent, irreducible, and aperiodic, the long-term sojourn times in four states (IDLEIDLE, IDLE, SUCCESS, COLLISION) of the SMP can be found as described in [26], obtaining:

$$\begin{cases} \Pi_{II}^c = \dfrac{1 \cdot \pi_{II}^c}{\pi_{II}^c + \pi_I^c + N\left(\pi_S^c + \pi_F^c\right)} = \dfrac{1}{1+(N+1)(1-\alpha)} \\ \Pi_I^c = \dfrac{1 \cdot \pi_I}{\pi_{II}^c + \pi_I^c + N\left(\pi_S^c + \pi_F^c\right)} = \dfrac{1-\alpha}{1+(N+1)(1-\alpha)} \\ \Pi_S^c = \dfrac{N\pi_S^c}{\pi_{II}^c + \pi_I^c + N\left(\pi_S^c + \pi_F^c\right)} = \dfrac{N\beta}{1+(N+1)(1-\alpha)} \\ \Pi_C^c = \dfrac{N\pi_C^c}{\pi_{II}^c + \pi_I^c + N\left(\pi_S^c + \pi_F^c\right)} = \dfrac{N(1-\alpha-\beta)}{1+(N+1)(1-\alpha)} \end{cases}$$

where the average sojourn times in the IDLEIDLE and IDLE states are equal to 1, while they are equal to N for the SUCCESS and FAILURE states.

Appendix C. Solving interconnected DTMCs and queues

C.1. Single-hop networks

In this scenario, there is a three-element coupling, between the channel DTMC, the tagged node DTMC and the tagged node Geo/G/1/L queue. This problem can be simplified through the following observations:

- the tagged node DTMC depends on π_0^n and p_i^c;
- the tagged node Geo/G/1/L queue depends on p_i^c;
- the channel DTMC depends on the distribution of the node DTMC through the parameter $p_{t|ii}^n$.

Eventually, the distributions of the interconnected DTMCs can be obtained by solving a fixed-point equation of the form:

$$p_i^c = \Phi(p_i^c) \tag{13}$$

where $\Phi(\cdot)$ is a proper rational function, which depends on the specific considered DTMCs. Therefore, we have a non-linear fixed-point equation. By deriving (univocally) the function $\Phi(p_i^c)$, the fixed point p_i^c corresponds to the intersection of the function $\Phi(p_i^c)$ with the bisector. We now propose another perspective on solving (13) which justifies the uniqueness of its solution.

In Fig. 14, we graphically describe the parameters which are passed among the tagged node block (DTMC and queue), and the channel DTMC. This iterative procedure can be summarized as follows.

1. The initial value of p_i^c is fixed at the output of the channel DTMC.
2. By using p_i^c, it is possible to solve the Geo/G/1/L queue at the tagged node and obtain π_0^n.
3. Given π_0^n and p_i^c, the tagged source DTMC can be solved and the corresponding probabilities $p_{t|ii}^n$ is passed to the channel DTMC.

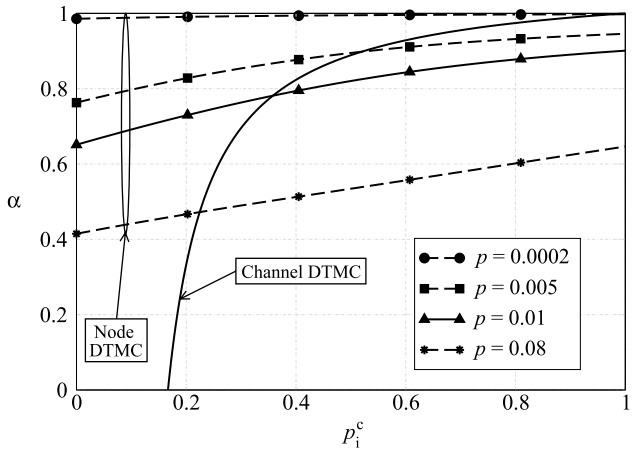

Fig. 15. For the tagged node block, the α is shown as a function of p_i^c, considering $L = 1$ and various values of p. For the channel DTMC, α is shown as a function of p_i^c.

4. Upon reception of $p_{t|ii}^n$, an updated value of p_i^c can be obtained at the output of the channel DTMC.
5. Step 2–4 are repeated until the value of p_i^c converges, i.e., there is no significant change over consecutive iterations.

In order to justify the existence and uniqueness of the solution p_i^c obtained through the proposed iterative method, we analyze separately the tagged node block (DTMC and queue) the channel DTMC. The tagged node block is such that, upon reception of p_i^c at its input, it outputs $p_{t|ii}$. In other words, this block can be characterized by a curve which describes $p_{t|ii}$ as a function of p_i^c. To be more precise, the probability $p_{t|ii}$ depends also on the traffic generation at the node, i.e., on the probability p. Therefore, for a generic value of p, a $p_{t|ii}$-p_i^c curve can be drawn. Similarly, the channel DTMC can be interpreted as a block which, upon, the reception of $p_{t|ii}$ at its input, outputs p_i^c. Therefore, this block can be characterized by a p_i^c-$p_{t|ii}$ curve. At this point, the obtained curves for the tagged node block and channel DTMC can be juxtaposed in the same graph. The iterative algorithm converges to an intersection point between these curves. Therefore, if only one intersection point between the two curves exists, one can conclude that the solution is unique. Since, as shown in Section 4.1.2, $\alpha = (1 - p_{t|ii})^M$, one can equivalently replace $p_{t|ii}^n$ by α and characterize the tagged node block and the channel DTMC with this parameter.

In Fig. 15, the output of the tagged node block probability α is shown, as a function of the probability p_i^c (output by the channel DTMC), in a scenario[7] with $L = 1$ and considering four values of the Bernoulli parameter p: (i) 0.0002, (ii) 0.005, (iii) 0.01, and (iv) 0.08. In the same figure, the α-p_i^c curve characterizing the channel DTMC is also shown. As one can see, for each value of p the intersection between the curves is unique and the iterative procedure, regardless of the starting point over one of these curves, converge to the unique solution. Therefore, we can conclude that the solution is unique and corresponds to the value of p_i^c of the unique intersection.

We now provide a more rigorous (mathematical) proof of the existence of the solution. The Brouwer theorem states that every continuous function from the unitary ball to itself has a fixed point [28]. In the considered network scenarios, the fixed-point equation (13) can be expressed as

$$\Phi\left(p_i^c\right) = \frac{2 - \alpha}{1 + (N + 1)(1 - \alpha)} \tag{14}$$

where $\alpha = (1 - p_{t|ii})^M$, and $p_{t|ii}$ is defined in Eq. (2) and, therefore, depends on p_i^c itself. One can observe that the value of p_i^c needs to be larger than $\frac{2}{2+N}$, since there are at least two empty slots because of the double CCA operations between two consecutive packet transmissions. Considering that p_i^c is a probability the domain and codomain of $\Phi\left(p_i^c\right)$ coincide with the closed real interval $[\frac{2}{2+N}, 1]$. It easy to verify that $\Phi\left(p_i^c\right)$ is also continuous, since it is a rational functional whose denominator is non-zero in the interval $[\frac{2}{2+N}, 1]$. However, the interval $[\frac{2}{2+N}, 1]$ is not a unitary ball and, therefore, the Brouwer theorem is not valid. In [28], one can find a generalization of the Brouwer theorem according to which a continuous function $\Phi : \mathcal{C} \to \mathcal{C}$ admits a fixed point if $\mathcal{C}$ is a compact convex finite-dimensional set. The interval $[\frac{2}{2+N}, 1]$ is a compact convex finite-dimensional set and, therefore, the fixed-point equation (14) has always a solution.

Once the existence of the solution has been proved, one should then prove its uniqueness. According to [28], the Eq. (14) admits a unique solution if $\Phi\left(p_i^c\right)$ is a contraction mapping[8] in the metric space $(\mathcal{C}, d)$, where d is a suitable metric, e.g., $d = |y - x|$ where $x, y \in \mathcal{C}$. In our case, the function

$$\Phi\left(p_i^c\right) : \left[\frac{2}{2+N}, 1\right] \to \left[\frac{2}{2+N}, 1\right]$$

[7] Similar considerations hold for a 1-hop scenario with a buffer length $L > 1$.

[8] Given a metric space $(\mathcal{C}, d)$, Φ is a contraction mapping if the minimum k such as $d(\Phi(x), \Phi(y)) \leq kd(x, y)\ \forall x, y \in \mathcal{C}$, is lower than one.

is a contraction mapping if Φ' exists and if $\sup|\Phi'| < 1$. Proving mathematically these two facts is not trivial, especially because of the large number of involved parameters, related to both the CSMA/CA MAC protocol (m, BE^{min} and BE^{max}) and the network structure (L, M, N and p). Therefore, we have just evaluated numerically the module of the derivative for the values of the system parameters considered in this work. In all cases, it holds that $\sup|\Phi'| < 1$. However, it can be verified that the function $\Phi\left(p_i^c\right)$ is not always monotonically increasing. Therefore, we cannot exploit this fact to formally prove the uniqueness of the solution, which, however, seems to hold according to the results shown in Fig. 15.

C.2. Multihop network scenarios

In Sections 4.2 and 4.3, it is shown how fixed-point equations can be derived to obtain the values of the parameters of interest, p_i^c and $\left\{p_r^{(k)}\right\}_{k=1}^{N_{relay}}$. However, in these cases as well one could extend the approach proposed in Appendix C.1 to derive an iterative algorithm to determine the unknown parameters p_i^c and $\left\{p_r^{(k)}\right\}_{k=1}^{N_{relay}}$, by passing proper probabilities between the tagged node block (DTMC and queue), relay blocks (DTMCs and queues), and the channel DTMC. In this case, multi-dimensional graphs should be considered and the intuitive visualization of the uniqueness of the solution is not straightforward. We are currently working on this extension.

References

[1] I. Akyildiz, W. Su, Y. Sankarasubramaniam, E. Cayirci, A survey on sensor networks, IEEE Commun. Mag. 40 (8) (2002) 102–114.
[2] IEEE 802.15.4 Std: Wireless Medium Access Control (MAC) and Physical MLayer (PHY) Specifications for Low-Rate Wireless Personal Area Networks (LR-WP ANs), IEEE Computer Society Press, 2003, 1–679.
[3] J. Zheng, M.J. Lee, A comprehensive performance study of IEEE 802.15.4, in: Wireless Sensor Network, John Wiley & Sons, New York, NY, USA, 2006, pp. 218–237 (Chapter 5).
[4] G. Ferrari, P. Medagliani, S.D. Piazza, M. Martalò, Wireless sensor networks: Performance analysis in indoor scenarios, EURASIP J. Wireless Commun. Network. (2007) 14 pages. doi:10.1155/2007/81864.
[5] I. Ramachandran, A.K. Das, S. Roy, Analysis of the contention access period of IEEE 802.15.4 MAC, ACM Trans. Sensor Netw. 3 (1) (2007) 29 pages.
[6] The Network Simulator (ns-2). Website, http://www.isi.edu/nsnam/ns/.
[7] H. Takagi, Queueing Analysis — A Foundation of Performance Evaluation. Volume III: Discrete-time Systems, North-Holland, Amsterdam, Holland, 1991.
[8] T. Wan, A.U. Sheikh, Performance and stability analysis of buffered slotted aloha protocols using tagged user approach, IEEE Trans. Vehicular Netw. 49 (2) (2000) 582–593.
[9] A. Sheikh, T. Wan, Z. Alakhdhar, A unified approach to analyze multiple access protocols for buffered finite users, J. Netw. Comput. Appl. 27 (2) (2004) 49–76.
[10] C.K. Singh, A. Kumar, P.M. Ameer, Performance evaluation of an IEEE 802.15.4 sensor network with a star topology, Wireless Network 14 (4) (2007) 543–568.
[11] S. Pollin, M. Ergen, S. Ergen, B. Bougard, L.D. Perre, I. Moerman, A. Bahai, P. Varaiya, F. Catthoor, Performance analysis of slotted carrier sense IEEE 802.15.4 medium access layer, IEEE Trans. Wireless Commun. 7 (9) (2008) 3359–3371.
[12] C.Y. Jung, H.Y. Hwang, D.K. Sung, G.U. Hwang, Enhanced Markov chain model and throughput analysis of the slotted CSMA/CA for IEEE 802.15.4 under unsaturated traffic conditions, IEEE Trans. Vehicular Netw. 58 (1) (2009) 473–478.
[13] J. He, Z. Tang, H.H. Chen, S. Wang, An accurate markov model for slotted csma/ca algorithm in IEEE 802.15.4 networks, IEEE Commun. Lett. 12 (6) (2008) 420–422.
[14] G. Bianchi, Performance analysis of the IEEE 802.11 distributed coordination function, IEEE J. Select. Areas Commun. 18 (3) (2000) 535–547.
[15] IEEE 802.11 Std: Wireless LAN Medium Access Control (MAC) a Physical Layer (PHY) Specifications, IEEE Computer Society Press, 1997, pp. 1–459.
[16] J. Mišic, V.B. Mišic, Queuing analysis of 802.15.4 beacon enabled PAN, in: Proc. of the IEEE/ACM First International Workshop on Broadband Wireless Services and Applications (BroadWISE), San Jose, CA, USA, 2004.
[17] Z. Tao, S. Panwar, G. Daqing, J. Zhang, Performance analysis and a proposed improvement for the IEEE 802.15.4 contention access period, in: Proc. IEEE Wireless Communications and Networking Conference, WCNC, vol. 4, 2006, pp. 1811–1818.
[18] J. Mišic, V.B. Mišic, Access delay for nodes with finite buffers in IEEE 802.15.4 beacon enabled PAN with uplink transmissions, Comput. Commun. 28 (10) (2005) 1152–1166.
[19] J. Mišic, S. Shafi, V.B. Mišic, Performance of a beacon enabled IEEE 802.15.4 cluster with downlink and uplink traffic, IEEE Trans. Parallel Distrib. Syst. 17 (4) (2006) 361–376.
[20] Z. Chen, C. Lin, H. Wen, H. Yin, An analytical model for evaluating IEEE 802.15.4 csma/ca protocol in low rate wireless application, in: IEEE Int. Conf. on Advanced Information Networking and Applications Workshop, AINAW, vol. 2, 2007, pp. 899–904.
[21] M. Martalò, G. Ferrari, S. Busanelli, Markov chain-based performance evaluation of IEEE 802.15.4 multihop wireless sensor networks, in: Proc. Third International Symposium on Communications, Control and Signal Processing, ISCCSP 2008, St. Julians, Malta, 2008, pp. 461–466.
[22] M. Martalò, S. Busanelli, G. Ferrari, Multihop IEEE 802.15.4 wireless networks with finite node buffers: Markov chain-based analysis, in: Proc. 10th International Symposium on Spread Spectrum Techniques and Applications, ISSSTA 2008, Bologna, Italy, 2008, pp. 644–648.
[23] J. Mišic, J. Fung, V.B. Mišic, Interconnecting 802.15.4 clusters in master-slave mode: queueing theoretic analysis, in: Proc. IEEE Int. Symposium on Parallel Architectures, Algorithms and Networks, ISPAN, Las Vegas, NA, USA, 2005, pp. 378–385.
[24] J. Mišic, R. Udayshankar, Slave-slave bridging in 802.15.4 beacon enabled networks, in: Proc. IEEE Wireless Communications and Networking Conference, WCNC, Hong Kong, China, 2007, pp. 3890–3895.
[25] H. Takagi, L. Kleinrock, Optimal transmission ranges for randomly distributed packet radio terminals, IEEE Trans. Commun. 32 (3) (1984) 246–257.
[26] V.G. Kulkarni, Modeling and Analysis of Stochastic Systems, Chapman and Hall, London, UK, 1995.
[27] Matlab Website, http://www.mathworks.com.
[28] V.I. Istratescu, Fixed Point Theory: An Introduction, Reidel Publishing Company, Dordrecht, Holland, 1981.

Marco Martalò was born in Galatina (LE), Italy, on June 1981. He received the "Laurea" degree (3-year program) and the "Laurea Specialistica" (3 + 2 year program) degree (summa cum laude) in Telecommunications Engineering on September 2003 and December 2005, respectively, from the University of Parma, Italy. On March 2009, he received the Ph.D. degree in Information Technologies at the University of Parma, Italy. From January 2009, he is a Post-Doc researcher at the Information Engineering Department of the University of Parma, Italy. From October 2007 to March 2008, he has been a "Visiting Scholar" at the School of Computer and Communication Sciences of the Ecole Polytechnique Federale De Lausanne (EPFL), Lausanne, Switzerland, collaborating with the laboratory of Algorithmic Research in Network Information, directed by Prof. Christina Fragouli. He is a member, at the Information Engineering Department of the University of Parma, Italy, of the Wireless Ad-hoc and Sensor Networks (WASN) Laboratory.

Martalò was a co-recipient of a "best student paper award" (with his tutor Dr. Gianluigi Ferrari) at the 2006 International Workshop on Wireless Ad hoc Networks (IWWAN'06). He has been TPC member of the International Workshop on Performance Methodologies and Tools for Wireless Sensor Networks (WSNPERF 2009) and the International Conference on Advances in Satellite and Space Communications (SPACOMM 2009). He also serves as a reviewer for many international journals and conferences.

Stefano Busanelli received the "Laurea" degree (3-year program) (summa cum laude) and the "Laurea Specialistica" (3 + 2 year program) degree (summa cum laude) in Telecommunications Engineering on 2004 and 2007, respectively, from the University of Parma, Italy. He is currently a Ph.D. student in Information Technologies at the Information Engineering Department of the University of Parma, Italy. From June 2008 to October 2008, he was an intern at Thales Communications (Colombes, France), working on cooperative wireless communications.

His main research interests include wireless sensor networks, vehicular ad hoc networks and cooperative relaying protocols.

Mr. Busanelli is a CNIT member and a GTTI student member.

Gianluigi Ferrari was born in Parma, Italy, in November 1974. He received the "Laurea" degree (five-year program) (summa cum laude) in electrical engineering and the Ph.D. degree in Information Technologies from the University of Parma in 1998 and 2002, respectively. From 2000 to 2001, he was a Visiting Scholar at the Communication Sciences Institute, University of Southern California, Los Angeles, CA, USA. Since 2002, he has been a Research Professor with the Department of Information Engineering, University of Parma, where he is now the coordinator of the Wireless Ad-hoc and Sensor Networks (WASN) Laboratory. Between 2002 and 2004, he visited several times, as a Research Associate, the Electrical and Computer Engineering Department at Carnegie Mellon University, Pittsburgh, PA. In fall 2007 he visited, as a DUO-Thailand Fellow, the King Mongkut's Institute of Technology Ladkrabang (KMITL), Bangkok, Thailand.

Ferrari has published more than 100 papers in leading international conferences and journals. He is coauthor of the books "Detection Algorithms for Wireless Communications, with Applications to Wired and Storage Systems" (Wiley: 2004), "Introduzione a Teoria della probabilità e variabili aleatorie con applicazioni all'ingegneria e alle scienze", (Editrice Esculapio-Progetto Leonardo:2008), "Ad Hoc Wireless Networks: A Communication-Theoretic Perspective" (Wiley: 2006), and "LDPC Coded Modulations" (Springer: 2009). He edited the book "Sensor Networks: where Theory Meets Practice" (Springer: 2009). His research interests include digital communication systems analysis and design, wireless ad hoc and sensor networking, adaptive digital signal processing, and information theory.

Ferrari is a co-recipient of a best student paper award at the 2006 International Workshop on Wireless Ad hoc Networks (IWWAN'06). He acts as a frequent reviewer for many international journals and conferences. He acts also as a technical program member for many international conferences. He currently serves on the Editorial Boards of "The Open Electrical and Electronic Engineering (TOEEJ) Journal" (Bentham Publishers), the "International Journal of RF Technologies: Research and Applications" (Taylor & Francis), and the "International Journal of Future Generation Communication and Networking" (SERSC: Science & Engineering Research Support Center).